Title

Acclimation of leaf photosynthesis and respiration to warming in field-grown wheat

Running Title

Acclimation to warming in field-grown wheat

Authors

Onoriode Coast[1,2*], Bradley C. Posch[1], Helen Bramley[3,] Oorbessy Gaju[1,4], Richard A. Richards[5], Meiqin Lu[6], Yong-Ling Ruan[7], Richard Trethowan[3,8] and Owen K. Atkin[1*]

Contact Information

[1]ARC Centre of Excellence in Plant Energy Biology, Research School of Biology, The Australian National University, Canberra, ACT 2601, Australia; [2]Natural Resources Institute, University of Greenwich, Central Avenue, Chatham Maritime, Kent ME4 4TB, United Kingdom; [3]School of Life and Environmental Sciences, Plant Breeding Institute, Sydney Institute of Agriculture, The University of Sydney, Narrabri, NSW 2390, Australia; [4]Lincoln Institute of Agri-Food Technology, University of Lincoln, Riseholme Park, Lincoln, Lincolnshire, LN2 2LG, United Kingdom; [5]CSIRO Agriculture and Food, GPO Box 1700, Canberra, ACT 2601, Australia; [6]Australian Grain Technologies, 12656 Newell Highway, Narrabri, NSW 2390, Australia; [7]Australia-China Research Centre for Crop Improvement and School of Environmental and Life Sciences, The University of Newcastle, Callaghan, NSW 2308, Australia; [8]School of Life and Environmental Sciences, Plant Breeding Institute, Sydney Institute of Agriculture, The University of Sydney, Cobbitty, NSW 2570, Australia.

*Corresponding authors:

Onoriode Coast (onoriode.coast@anu.edu.au; https://orcid.org/0000-0002-5013-4715)

Owen K. Atkin (owen.atkin@anu.edu.au; https://orcid.org/0000-0003-1041-5202)

Additional Authorship Options

Onoriode Coast and Bradley C. Posch should be considered joint first author.

Funding

ARC Centre of Excellence in Plant Energy Biology (CE140100008)

Grains Research and Development Corporation, National Wheat Heat Tolerance Project (US00080)

Abstract

Climate change and future warming will significantly affect crop yield. The capacity of crops to dynamically adjust physiological processes (i.e. acclimate) to warming might improve overall performance. Understanding and quantifying the degree of acclimation in field crops could ensure better parameterization of crop and Earth System models and predictions of crop performance. We hypothesized that for field-grown wheat, when measured at a common temperature (25°C), crops grown under warmer conditions would exhibit acclimation, leading to enhanced crop performance and yield. Acclimation was defined as: (i) decreased rates of net photosynthesis at 25°C (A^{25}) coupled with lower maximum carboxylation capacity ($V_{cmax}{}^{25}$); (ii) reduced leaf dark respiration at 25°C (both in terms of O_2 consumption, $R_{dark}\_O_2{}^{25}$; and CO_2 efflux, $R_{dark}\_CO_2{}^{25}$); and (iii) lower $R_{dark}\_CO_2{}^{25}$:$V_{cmax}{}^{25}$. Field experiments were conducted over two seasons with 20 wheat genotypes, sown at three different planting dates, to test these hypotheses. Leaf-level CO_2 based traits (A^{25}, $R_{dark}\_CO_2{}^{25}$, and $V_{cmax}{}^{25}$) did not show the classic acclimation responses that we hypothesized; by contrast, the hypothesized changes in $R_{dark}\_O_2$ were observed. These findings have implications for predictive crop models that assume similar temperature response among these physiological processes, and for predictions of crop performance in a future warmer world.

Key words:

Acclimation, climate change, heat stress, dark respiration, wheat

Introduction

Anthropogenic activities have increased atmospheric CO_2 concentration resulting in global warming. Earth System Models (ESMs) predict that average annual global land surface temperatures will rise by 0.3–4.8°C by 2100 (Collins et al., 2013). This increase in temperature is likely to affect the growth of plants in natural and managed ecosystems, with the effect of climate change on crops being of particular importance. Understanding how key physiological processes in crops – particularly leaf photosynthesis and respiration - respond to rising temperatures, including quantifying their capacity to thermally acclimate, will be critical for global food security (Lobell & Gourdji, 2012) and modelling crop responses to climate change (Huntingford et al., 2017; Smith & Dukes, 2013; Wang et al., 2017).

Leaf dark respiration [$R_{dark,}$ defined either as non-photorespiratory mitochondrial CO_2 release in darkness ($R_{dark}\_CO_2$) or dark O_2 consumption ($R_{dark}\_O_2$)] and photosynthesis (net CO_2 assimilation rate, A) differ in their response to temperature. Short-term (minutes to hours) elevations in temperature induce a near-exponential increase in R_{dark} (Atkin & Tjoelker, 2003) up to a maximum at around 50–60°C, followed by a rapid decline in R_{dark} indicating irreversible damage to the respiratory apparatus (O'Sullivan et al., 2013). For net photosynthesis, A increases in response to short-term elevations in temperature until it reaches its optimum (often in the 25–35 °C range) and then decreases at supra-optimal temperatures. Under long-term (several days or longer) warming, plants dynamically adjust (i.e. acclimate) rates of A and R_{dark} to maintain fixation of CO_2 and/or limit CO_2 release, respectively. Acclimation to long-term warming should improve plant performance through constructive adjustment that maximise daytime net CO_2 assimilation and minimize daily respiratory CO_2 loss (Way & Yamori, 2014). Most studies that have shown beneficial effects of adjustment on plant performance have been

for acclimation to light in non-crop plants (Athanasiou, Dyson, Webster, & Johnson, 2010; Frenkel, Bellafiore, Rochaix, & Jansson, 2007). The opposite of constructive adjustment is detractive adjustment such as unsustainable increase in rates of R_{dark} or decline in rates of photosynthesis of warmed plants at high temperature, which does not improve a plant's ability to grow and/or survive in its new growth regime (Slot & Winter, 2016; Way & Yamori, 2014). It remains unknown whether annual field crops respond to temperature through constructive adjustment.

Acclimation to elevated temperatures might be partial or full, the latter potentially leading to reset of metabolic homeostasis , when cool and warm grown plants are compared at their respective growth temperatures. Acclimation of R_{dark} to sustained warming is characterised by decreases in R_{dark}'s temperature sensitivity (e.g. Q_{10}, the proportional change in R_{dark} per 10°C change in temperature; Type I acclimation) or the downward regulation of the basal rate of R_{dark} at a reference temperature (e.g. at 25°C, R_{dark}^{25}; Type II acclimation) or a combination of both (Atkin & Tjoelker, 2003). Altered Q_{10} values reflect changes in the underlying factors regulating respiratory flux (e.g. substrate availability and/or the turnover of ATP to ADP) (Atkin & Tjoelker, 2003). Type II acclimation is likely underpinned by decreases in respiratory capacity associated with changes in mitochondrial abundance, structure and/or protein composition (Anna, Logan, & Atkin, 2006; Campbell et al., 2007; Rashid et al., 2020). For photosynthesis, growth under warm conditions is characterised by a number of changes (relative to plants grown at lower temperatures) including: lower rates of A measured at temperatures below the thermal optimum of A (i.e. leaf temperature where maximal rates of A occur); higher or similar rates of A at the thermal optimum (Way & Yamori, 2014); an increase in the leaf temperature at which the thermal optimum of A occurs (Berry & Bjorkman, 1980); and, a down-regulation of photosynthetic capacity (maximum carboxylation rate, V_{cmax} and/or

maximum electron transport rate, J_{max}), when measured at a set temperature (e.g. V_{cmax} at 25°C, V_{cmax}^{25}) (Ghannoum et al., 2010). For plants that are growing near or above their optimum temperature, the downregulation of V_{cmax}^{25} can lead to decreases in daily net CO_2 uptake (Way & Sage, 2008) that may compromise plant performance.

The greatest source of uncertainty in models used to simulate the impact of climate change on crop yields (Bassu et al., 2014; Li et al., 2015; Rosenzweig et al., 2013; Wang et al., 2017) is attributed to contrasting differences in the temperature response functions of key physiological processes (Senthold Asseng et al., 2013; Wang et al., 2017). Most models assuming a fixed temperature response of key physiological processes. In many ESMs, R_{dark} is modelled from A or V_{cmax}. For example, in MOSES-TRIFFID (now JULES), BIOME3, and BETHY, R_{dark} is estimated to be 0.011-0.015 (for C_3 plants) or 0.025-0.042 (for C_4 plants) of V_{cmax} at a common temperature of 25°C (Cox, 2001; Haxeltine & Prentice, 1996; Knorr, 2000; Ziehn, Kattge, Knorr, & Scholze, 2011). But R_{dark}^{25}:V_{cmax}^{25} varies between cold and hot acclimated plants. A global study of 899 species across 100 sites from the tropics, reported greater R_{dark}:V_{cmax} in species at cold sites compared to species at warmer sites, with faster rates of R_{dark}^{25} at a given V_{cmax}^{25} for C_3 herbs/grasses compared with broadleaved/needle-leaved plants and shrubs (Atkin et al., 2015). These acclimation responses and the change in R_{dark}^{25}:V_{cmax}^{25} are rarely accounted for by models when predicting crop responses under warmer field conditions (Li et al., 2015). One reason for this deficiency in crop models is in part due to the difficulty in obtaining relevant field data for model evaluation. The extent to which acclimation changes R_{dark}^{25}:V_{cmax}^{25} in crops grown under thermally contrasting field settings remains untested.

125 Wheat is an ideal annual crop species for examining the acclimation response of leaf
126 R_{dark} and A to warming and its relationships with plant performance (or crop yield) under
127 realistic field settings. There is increasing evidence that warming in many wheat producing
128 regions (including China, India, USA, France and Australia) is resulting in either stalled or
129 reduced wheat yields (Hochman, Gobbett, & Horan, 2017; Zhao, Li, Yu, Cheng, & He, 2016).
130 Some of the ways that warming can affect crop yield include accelerating phenological
131 development, consequently shortening the time available for crops to efficiently capture and
132 convert natural resources into yield (Slafer & Rawson, 1994); altering the rates of R_{dark} (Atkin
133 & Tjoelker, 2003) and A (Crafts-Brandner & Salvucci, 2002; Sage & Kubien, 2007), potentially
134 reducing daily net CO_2 uptake; reducing A due to stomatal closure with increasing atmospheric
135 vapour pressure deficit (Lin, Medlyn, & Ellsworth, 2012); and, directly disrupting reproductive
136 development leading to floral and grain abortion (Ruan, Patrick, Bouzayen, Osorio, & Fernie,
137 2012). Although genotypic variation exists for wheat sensitivity to high temperature, the degree
138 of variation in acclimation of leaf R_{dark} and A to warming is unknown.

139 Our understanding of acclimation responses to warming has improved over time (Atkin
140 & Tjoelker, 2003; Berry & Bjorkman, 1980; Hikosaka, Ishikawa, Borjigidai, Muller, & Onoda,
141 2006; Larigauderie & Körner, 1995; Sage & McKown, 2006; Way & Yamori, 2014). This gain
142 has come from experiments predominantly conducted either in temperature-controlled settings
143 or by exploiting natural temperature variations. Some examples of the latter include studies
144 conducted along regional climatic gradients or across different seasons (Drake et al., 2015;
145 Tjoelker, Oleksyn, Reich, & Żytkowiak, 2008). Another example involves the use of different
146 times of sowing (TOS) within a cropping season. The TOS concept is commonly used by crop
147 modelers and agronomists as a surrogate for generating different thermal environments in
148 studies of crop responses to temperature (Hunt et al., 2019; Kirkegaard et al., 2016; Wang et

al., 2019). Adjusting TOS has also been suggested as one of the most convenient management strategies for climate change impact at the field level (Donatelli, Srivastava, Duveiller, Niemeyer, & Fumagalli, 2015). While its use is complicated by the difficulty in isolating the effect of temperature from other environmental factors, adjusting TOS can nonetheless, provide insights into the response of crops to changes in growth temperature under typical field conditions.

Considering the points described above, we used wheat crops sown on three planting dates (three TOS) and two cropping seasons to test if the assumption of fixed temperature responses of R_{dark} and A with temperature used in crop and Earth System models (Cox, 2001; Hansen, Jensen, Nielsen, & Svendsen, 1991; Oleson et al., 2013; Ruimy, Dedieu, & Saugier, 1996) holds true for wheat. We hypothesized that, when measured at a commonly reported standardized temperature of 25°C, plants grown under warmer field settings would – relative to cooler grown plants - show: (i) decreased leaf A^{25} coupled with lower $V_{cmax}{}^{25}$ due to acclimation to higher growth temperature; (ii) lower leaf $R_{dark}{}^{25}$ when measured on both O_2 and CO_2 bases, i.e. exhibit a downward shift in the R_{dark}-temperature response curve due to acclimation; and (iii) lower $R_{dark}\_CO_2{}^{25}$:A^{25} and $R_{dark}\_CO_2{}^{25}$:$V_{cmax}{}^{25}$. We normalised measurements to 25°C, which is close to the optimum temperature of 27.5°C for A in wheat (Wang et al., 2017). To quantify the extent to which acclimation of leaf R_{dark} was Type I or Type II (Atkin and Tjoelker 2003), we estimated short-term temperature responses of R_{dark} at anthesis of TOS 1-3 plants. Finally, we examined if the temperature response of leaf R_{dark} and A at anthesis was reflective of overall crop performance at harvest.

Materials and methods

Experimental sites

Two field experiments were conducted over a 2-year period to investigate variation in acclimation to temperature of R_{dark} and A^{25} of wheat. The experiments were located in commercial wheat farms in Dingwall (35°48'22.2" S, 143°47'3.3" E) and Barraport West (36°2'38.6" S, 143°32'20.9" E), Victoria, Australia, during the spring of 2017 and 2018, respectively. Dingwall and Barraport West are 49 km apart but both in the Mallee district of the SE region of Australia. Soils within the region are relatively infertile (Isbell, 1996).

Plant materials and growing conditions

The trials consisted of 20 wheat genotypes, including four commercial cultivars (Corak, Trojan, Mace, and Suntop) and 16 breeding lines developed by the University of Sydney's Plant Breeding Institute for the Australian environment (Table S1). The 16 breeding lines cover a diverse genetic background, including hexaploid genotypes derived from crosses to emmer wheat-based hexaploid lines (*Triticum dicoccon* Schrank ex Schübl.) (Ullah et al., 2018) and genotypes with pedigrees originating from hot climates, such as Sudan, India and Mexico. Seeds were sown on three dates in 2017 (02 May, 02 June and 01 July) and 2018 (09 May, 01 June and 03 July) in order to expose crops to different growth temperatures at a common developmental stage. The first times of sowing (TOS) for both experiments were within the locally recommended periods for sowing. For brevity, the first, second and third TOS will henceforth be referred to as TOS1, TOS2 and TOS3, respectively.

The 2017 and 2018 experiments conducted primarily under rainfed conditions, with supplemental watering provided by an overhead centre pivot (2017) or overhead lateral move

192 (2018) irrigator. Rainfall and irrigation at both sites are given in Table S3. The trials were
193 managed by the Birchip Cropping Group (BCG; www.bcg.org.au) following standard
194 agronomic practices for the region. Daily maximum and minimum temperatures, and rainfall
195 data were obtained from the closest Australian Bureau of Meteorology (BOM) weather station,
196 which was ~0.7 km from the experimental site, for the first 140 days after sowing (DAS) for
197 Experiment I. From 141 DAS onwards in 2017 and throughout 2018 a weather station was
198 placed on site to record temperature, relative humidity, rainfall, solar radiation and
199 evapotranspiration at 15-minute intervals.

200 *Experimental design*

201 The experiments were sown using a 6-row planter at a rate of 130 plants m^{-2} and each row
202 spaced 30 cm apart. Each experiment was sown as three adjacent fields, one for each TOS.
203 Each field consisted of four replicate blocks and each block had 20 plots that were 2.15 x 4 m.
204 Individual fields were buffered on all sides with the commercial cultivar Mace using the same
205 spacing and plant density as in the plots. The wheat lines were randomly allocated to the plots
206 using Digger biometrics software (http://nswdpibiom.org/austatgen/software/). Samples for
207 physiological measurements were collected from plants in rows 3 or 4 of plots.

208 *Measurement of physiological traits*

209 All physiological measurements were carried out at Zadok growth scale between 59-70
210 (Zadoks, Chang, & Konzak, 1974; when about 50% of plants in each TOS were between early
211 and late flowering). In 2017, measurements were conducted over three-day periods on 26–28
212 September (147–149 DAS) for TOS1, 17–19 October (137–139 DAS) for TOS2 and 24–26
213 October (115–117 DAS) for TOS3. In 2018, measurements were made on 03–05 October (147–

149 DAS) for TOS1, 17–19 October (138–140 DAS) for TOS2 and 30 October–01 November (119–121 DAS) for TOS3. In both 2017 and 2018, leaf $R_{dark}\_O_2^{25}$ of all 20 genotypes were completed over two days, with two replicates sampled on the first day and two replicates on the second. Flag leaves were harvested between 0830 and 1030 h. Samples were stored temporarily for at least 30 minutes in cool, moist darkened containers prior to sample preparation and measurements for dark adaptation. Measurements were concluded within 6 h of harvesting leaves.

Measurement of A^{25} and $R_{dark}\_CO_2^{25}$: Leaf CO_2 gas exchange measurements were limited to six genotypes, which included the two commercial cultivars Mace and Suntop. Unpublished data from previous studies show that these six lines were representative of the diversity of the set of 20 lines. Leaf CO_2 gas exchange measurements were conducted for all TOS in 2017 and 2018. Leaf A^{25} and $R_{dark}\_CO_2^{25}$ were measured using Licor 6400XT Portable Photosynthesis Systems (Li-6400XT, Licor, Lincoln, NE, USA). Licor units with a 6 cm^2 leaf chamber and red-blue light source (6400-18 RGB Light Source, Licor) were used, with the chamber temperature set to 25°C, reference line atmospheric [CO_2] to 400 ppm and a flow rate of 500 μmol s^{-1}. Flag leaves of the main stems, from one plant per plot, were used for all measurements. To determine A^{25}, leaves in chambers were exposed to saturating irradiance of 1500 μmol photons m^{-2} s^{-1} for at least five min, after which A^{25} was measured following equilibrium (stable readings for at least one minute). Immediately after measuring A^{25}, light within the chamber was turned off and leaves dark adapted for at least 30 min (to avoid post-illumination transients; Atkin, Evans, and Siebke (1998); Azcon-Bieto, Day, and Lambers (1983)) then $R_{dark}\_CO_2^{25}$ was measured. Relative humidity (RH) within the chamber was

maintained between 40 and 75% for all measurements. These measurements were taken within a day between 0900 and 1730 h (~40 min before sunset) for each TOS.

Estimates of V_{cmax} using the *'one-point-method'*: To assess whether TOS influenced net photosynthetic rates (A) in the absence of limitations in stomatal conductance (and thus limitations in C_i), we estimated the catalytic capacity of Rubisco (V_{cmax}) using the 'one-point method' (Wilson, Baldocchi, & Hanson, 2000), which was recently validated by (De Kauwe et al., 2016). These V_{cmax} values were then used to obtain estimates of A at a set internal CO_2 concentration (C_i) of 250 ppm (De Kauwe et al., 2016), using Eqn 1:

$$V_{cmax} = A_{sat} + R_{light} (C_i + K_c[1 + O/K_o]) / (C_i - \Gamma^*) \quad \text{Eqn 1}$$

where Γ* is the CO_2 compensation point in the absence of nonphotorespiratory mitochondrial CO_2 release (36.9 µbar at 25°C), O is the partial pressure of oxygen (kPa), C_i is the intercellular CO_2 partial pressure (Pa), R_{light} is the rate of nonphotorespiratory mitochondrial CO_2 release (here assumed to be equal to $R_{dark\_}CO_2^{25}$), and K_c (59.4 kJ mol^{-1}) and K_o (36 kJ mol^{-1}) are the Michaelis–Menten constants (K_m) of Rubisco for CO_2 (404 µbar) and O_2 (248 mbar), respectively, at 25°C (Evans, von Caemmerer, Setchell, & Hudson, 1994; von Caemmerer, Evans, Hudson, & Andrews, 1994). Using this approach, we assumed that A at saturating irradiance and ambient CO_2 is limited by Rubisco carboxylation rather than by ribulose 1,5-bisphosphate (RuBP) regeneration. Moreover, we assumed that leaf mitochondrial respiration in the light (R_{light}) can be equal to those measured on the same leaf in darkness. Because leaf temperatures were not always at 25°C during gas exchange measurements we standardized V_{cmax} to 25°C (V_{cmax}^{25}) following:

$V_{cmax}^{25} = V_{cmax} / [\exp((T - 25) * \Delta E_a) / (R * 298(T + 273.15)))]$ Eqn 2

where T is the leaf temperature at which A was measured (and V_{cmax} was initially estimated), ΔE_a is the activation energy [assuming = 64.8 kJ mol^{-1}, Badger and Collatz (1977)], and R is the universal gas constant (8.314 J mol^{-1} K^{-1}).

Leaf $R_{dark}\_O_2$: For all 20 genotypes, four 4 cm^2 sections of flag leaf tissue from one stem per plot, cut from the middle of the leaf, were used to estimate flag leaf $R_{dark}\_O_2$ at 20, 25, 30 and 35°C. Measurements were taken using an automated Q_2 O_2-sensor (Astec Global, Maarssen, the Netherlands) described in Scafaro et al. (2017) and previously used for wheat (Coast et al., 2019).

Leaf traits: Leaf mass per unit area (LMA) and leaf N were determined using leaf sections covered within the cuvette of the Licor head during the gas exchange measurements. The leaf sections were oven-dried at 60°C for 72 h then weighed. The same leaf sections were used to determine leaf N content (%), by combustion using a Carlo-Erba elemental analyser (NA1500, Thermo Fisher Scientific, Milan, Italy). Leaf N content and LMA were used to estimate leaf N per unit dry mass (N_{mass}) and N per unit leaf area (N_{area}).

Yield: At harvest maturity when grain moisture was approximately 9–11%, all plots (each 8.6 m^2) were harvested using a combine harvester. Final yield of each plot was determined based on machine harvests of three adjacent inner rows. Grain yield measured in grams per plot was converted to tonnes per hectare and used for all analyses.

Statistical analysis

The 2017 and 2018 experiments were treated as different experiments and their data analysed separately. We conducted ANOVA on all physiological variables, leaf traits and ratios of

279 $R_{dark}\_CO_2^{25}$ to A^{25} and V_{cmax}^{25} using the General Treatment Structure in Randomized Blocks
280 Design function in GENSTAT (18th edn, VSN International Ltd, Hemel Hempstead, UK).
281 Genotype, TOS and their interaction term were taken as the treatment terms and block as the
282 replicate term. Means were separated by l.s.d. (P=0.05, unless otherwise stated).

283 Slopes of log-transformed temperature response curves (20–35°C) of $R_{dark}\_O_2$ were
284 used to compute Q_{10}. To assess the type of acclimation of $R_{dark}\_O_2$ that occurred we compared
285 the slopes of the log R_{dark}-temperature response curves. Lower slopes for TOS2 and TOS3
286 compared to TOS1 would indicate Type I acclimation; the absence of significantly lower slopes
287 but lower intercepts for TOS2 and TOS3 would indicate Type II acclimation (Slot & Kitajima,
288 2015).

289 Relationships of leaf physiological characteristics (A^{25}, $R_{dark}\_CO_2^{25}$ and $R_{dark}\_O_2^{25}$)
290 with LMA, N_{mass} and N_{area} or measured environmental variables were explored using bivariate
291 and multiple linear regressions. The measured environmental factors were daily average
292 minimum temperature (T_{min}) or maximum temperature (T_{max}) over the 1–10 day period before
293 50% of plants had achieved anthesis (DBA) and 1–3 day period when 50% of plants were at
294 anthesis (DAA). Other measured variables were mean photosynthetically active radiation and
295 total solar radiation during the 1–3 DAA. To test if TOS or experiments influenced these
296 relationshsips, analyses were initially conducted separately for 2017 and 2018 and later with
297 data from both experiments combined. Multiple linear regressions were also conducted to
298 explain variation in grain yield by measured and estimated leaf traits. Stepwise regression was
299 used to select the best-fitting equation given the set of input leaf traits.

Results

Environmental conditions during vegetative growth and at anthesis

From sowing to anthesis, average T_{min} and T_{max} were similar for TOS1 and TOS2 across the two experiments, but Tmax of TOS3 was warmer in 2018 than 2017 (Table 1). During the 1–3 DAA period, T_{min} was generally warmer in 2017 than in 2018. Rainfall between sowing and anthesis was 19–44% higher in 2017 compared to 2018 (Table 1 and S2). Rainfall was supplemented by irrigation, with less irrigation (in terms of quantity and application times) and overall water supplied to 2017 (Table S3). However, the combination of rainfall and irrigation provided sufficient moisture to the plants except for a brief period of water deficit stress (with visible signs of leaf rolling) during the period of physiological measurements for TOS2 and just prior to that of TOS3 for 2018. This is not reflected in total water supplied (Supplementary Table S3). The sum of daily solar radiation from sowing to anthesis was 477–502 kWh m^{-2} in Experiment I, with this range being narrower than that for 2018 which was 420–606 kWh m^{-2}.

During the 1–3 DAA period T_{min}/T_{max} of TOS2/TOS3 were warmer than TOS1 by 6–10°C in 2017 and 1–10°C in 2018. Total solar radiation was 4–5 kWh m^{-2} more and photosynthetically active radiation was 60–160% higher in TOS2/TOS3 than TOS1 for 2017 (Table 1). For the same period of 2018, T_{min} of TOS2/TOS3 were approximately 2°C warmer than TOS1, T_{max} of TOS3 was more than 10°C warmer than TOS1, and solar radiation was 4–5 kWh m^{-2} more in TOS2/TOS3 than for TOS1. Mean photosynthetically active radiation of the three TOS for 2018 were about the same (Table 1).

Temperature responses of leaf CO_2 exchange among six wheat genotypes

For Experiment I, there was no significant genotype by TOS interaction effects (P>0.05) on leaf A^{25}, V_{cmax}^{25} or $R_{dark}\_CO_2^{25}$ (Table 2) but all three variables were significantly greater under TOS2 and TOS3 compared with TOS1 (Fig. 1, Table 2). Mean leaf A^{25} was significantly higher (P<0.001) by 10% for TOS2 and 23% for TOS3 than TOS1. Stomatal conductance mirrored the increases with TOS seen in leaf A^{25}, with mean values being 0.24 mmol m^{-2} s^{-1} at TOS1, 0.31 mmol m^{-2} s^{-1} at TOS2 and 0.41 mmol m^{-2} s^{-1} at TOS3 (i.e. 34–67% higher, P<0.001). Similarly, V_{cmax}^{25} and leaf $R_{dark}\_CO_2^{25}$ were 11–46% and 15–18% greater at TOS2 and TOS3 compared with TOS1 (Fig. 1c, e). Genotypes only differed for V_{cmax}^{25}, there were no other significant genotype effects (Table 2).

There was no significant genotype x TOS effect for A^{25} and $R_{dark}\_CO_2^{25}$ in 2018, consistent with 2017 (Table 2). However, TOS responses of leaf A^{25} and $R_{dark}\_CO_2^{25}$ for 2018 were not consistent with those of 2017 (Fig. 1). Mean leaf A^{25} reduced in TOS2 and TOS3 compared with TOS1. The reduction was greater in TOS2 than TOS3 due to lower stomatal conductance. Mean stomatal conductance for TOS2 at 0.064 mmol m^{-2} s^{-1} and TOS3 at 0.098 were 56 and 33% less (P<0.001) than that of TOS1 (0.145 mmol m^{-2} s^{-1}), respectively. The reduced stomatal conductance was in response to apparent water deficit stress during the period of physiological measurement for TOS2. However, estimates of V_{cmax}^{25} showed consistent increases (46–55%) from TOS1 to TOS2 and TOS3 (Fig. 1d). Compared with TOS1, leaf $R_{dark}\_CO_2^{25}$ increased slightly at TOS2 but was similar at TOS3 (Fig. 1f). As was the case for Experiment I, there was no significant effect of genotype on leaf A^{25} and $R_{dark}\_CO_2^{25}$ in 2018, but there was for V_{cmax}^{25} (Table 2).

Temperature responses of leaf $R_{dark}\_O_2$ across 20 wheat genotypes

343 Leaf $R_{dark}\_O_2^{25}$ of the six selected genotypes were representative of the whole set of 20
344 genotypes (Fig. 2). Generally, leaf $R_{dark}\_O_2^{25}$ reduced in TOS2 and TOS3 compared to TOS1
345 in Experiment I, whereas for 2018 there was no significant difference among the three TOS
346 (Fig. 2). There was neither genotype effect nor genotype by TOS interaction on leaf $R_{dark}\_O_2^{25}$
347 for the six or 20 genotypes (Table 2). However, leaf $R_{dark}\_O_2$ of all 20 genotypes and at the
348 other three measurement temperatures (20, 30 and 35°C) revealed differences which were not
349 apparent with just the selected six genotypes at 25°C. For example, while there was no TOS
350 effect on leaf $R_{dark}\_O_2$ at 25°C in 2018, measurements at 20, 30 and 35°C showed highly
351 significant differences among TOS (Fig. 3).

352 Regression of log transformed leaf $R_{dark}\_O_2$ by measurement temperature showed
353 substantial genotypic and TOS variation for both 2017 and 2018 (Fig. 3, Tables S4 and S5).
354 For both experiments, TOS1 had higher $R_{dark}\_O_2$ than TOS2 and TOS3 (Fig. 3), and
355 significantly different slopes or intercepts from TOS2 and TOS3 (Table S6). In Experiment I,
356 across all times of sowing, Q_{10} values of the different genotypes ranged from 2.03–2.64 (Table
357 S4), and across all genotypes TOS1 exhibited the lowest Q_{10} (Fig. 3a). For 2018, the range of
358 Q_{10} for the genotypes was 1.85–2.53 (Table S5). Across genotypes, TOS1 had a higher Q_{10}
359 than TOS3 but not statistically different from TOS2 (Fig. 3b).

360 *Relationship of wheat leaf photosynthetic and respiratory traits with growth temperatures and*
361 *other environmental factors.*

362 For Experiment I, A^{25} and V_{cmax}^{25} were significantly associated with T_{max} during the 1-10 DBA
363 and T_{min} of the 1–5 DBA (for A^{25}) or 1–3 DBA (for V_{cmax}^{25}; Fig. 4). Mean rate of A^{25} increased
364 with increasing pre-anthesis growth temperature with the rate of the increase greater for night-
365 time temperatures than day-time. Leaf $R_{dark}\_CO_2^{25}$ was positively associated with anthesis T_{max}

366 and T_{min} with close to 50% of the variation explained by the growth temperature. Including
367 photosynthetically active radiation and/or solar radiation in the regression models of leaf A^{25}
368 or $R_{dark}\_CO_2^{25}$ with, T_{min} and T_{max} did not result in better goodness of fits than without the
369 parameters included (data not shown). Leaf $R_{dark}\_O_2^{25}$ was associated with T_{min} and T_{max} of the
370 1–3 DAA, decreasing with rise in growth temperature (Fig. 5). The relationship of $R_{dark}\_O_2$
371 over the 1–3 DAA period was weaker with photosynthetically active radiation (r^2=0.33–0.40),
372 in a broader but similar range to that with solar radiation (r^2=0.44–0.69) or all four
373 environmental variables combined (r^2=0.54–0.69).

374 For 2018, the strength of the associations of these leaf traits with T_{min} or T_{max} were of
375 the order A^{25}> $R_{dark}\_CO_2^{25}$> $R_{dark}\_O_2^{25}$. The slopes and intercepts that describe the relationships
376 of the leaf traits with T_{min} and T_{max} were significant and different. Leaf A^{25} and $R_{dark}\_O_2$
377 decreased with T_{min} or T_{max}, while $R_{dark}\_CO_2^{25}$ increased with T_{min} only (no significant
378 relationship vs T_{max}; Fig. 4 and 5). The slope of the A^{25} vs T_{min} or T_{max} regression was higher
379 for T_{max} than T_{min}, whereas that for leaf R_{dark}^{25} was steeper for T_{min} than T_{max} (Fig. 4 and 5).

380 Across genotypes, TOS and experiments, multiple linear regression models with
381 combined T_{min}, $T_{max,}$ photosynthetically active radiation and solar radiation of the 1–3DAA
382 accounted for 72 and 25%, respectively, of the variation in wheat flag leaf A^{25}, and $R_{dark}\_CO_2^{25}$.
383 For $R_{dark}\_O_2$ (depending on the measurement temperature) the variation accounted for was 40–
384 48% for all 20 genotypes or 39–64% for the six genotypes (Table S7).

385 *Acclimation of $R_{dark}\_CO_2^{25}$:A^{25} and $R_{dark}\_CO_2^{25}$:V_{cmax}^{25} among six wheat genotypes*

386 The asynchronous degree and/or direction of the response of $R_{dark}\_CO_2^{25}$ and A^{25} or V_{cmax}^{25} to
387 TOS resulted in significant changes in the ratios of $R_{dark}\_CO_2^{25}$:A^{25} and $R_{dark}\_CO_2^{25}$:V_{cmax}^{25} with
388 change in TOS in both Experiments (Table 3). The general pattern was one of consistent

389 reductions in the ratios when comparing TOS3 vs TOS2, and less so for TOS3 vs TOS1 or
390 TOS2 vs TOS1. In Experiment I, $R_{dark}\_CO_2^{25}$:A^{25} and $R_{dark}\_CO_2^{25}$:V_{cmax}^{25} reduced by 19 and
391 31%, respectively, from TOS2 to TOS3 (Table 3). In 2018, $R_{dark}\_CO_2^{25}$:A^{25} of TOS3 was 52%
392 lower compared to TOS2. Between TOS3 and TOS1, the differences in the ratios varied, from
393 significant reduction for $R_{dark}\_CO_2^{25}$:V_{cmax}^{25} irrespective of the experiment, to marginally
394 different for $R_{dark}\_CO_2^{25}$:A^{25} in 2017 and no difference for $R_{dark}\_CO_2^{25}$:A^{25} in 2018 (Table 3).

395 *Leaf trait-trait relationships among six wheat genotypes*

396 There were significant variations in leaf N and LMA in both experiments with genotype or
397 TOS (Table S8). In 2017 and 2018, bivariate relationships between leaf physiological traits
398 (A^{25}, $R_{dark}\_CO_2^{25}$ and $R_{dark}\_O_2^{25}$) and chemical (N_{area} and N_{mass}) or morphological (LMA) traits,
399 expressed on either an area- or mass-basis, were not significantly altered by TOS (in terms of
400 differences in both slope and intercepts from TOS1). The only exceptions were: mass-based
401 $R_{dark}\_O_2^{25}$ vs LMA of TOS2 in 2017 (Table S9); area-based A^{25} vs N_{area} for TOS2 in 2018; and
402 mass-based $R_{dark}\_CO_2^{25}$ vs LMA of TOS2 in 2017 (Table S10). In 2017 and 2018, and across
403 both experiments, singular regressions of LMA, N_{area}, N_{mass} or V_{cmax}^{25} with A^{25}, $R_{dark}\_CO_2^{25}$ or
404 $R_{dark}\_O_2^{25}$ were in most cases significant but also weak (r^2=0.05–0.29). Across experiments,
405 the strongest bivariate relationship (in terms of r^2) for A^{25} or $R_{dark}\_CO_2^{25}$ was with LMA when
406 A^{25} or $R_{dark}\_CO_2^{25}$ was expressed per leaf area (Fig. S1–S3). Leaf N, V_{cmax}^{25} and LMA were
407 better correlated with A^{25}, $R_{dark}\_CO_2^{25}$ or $R_{dark}\_O_2^{25}$ when combined than when treated
408 independently (Table S11). However, the addition of V_{cmax}^{25} to regressions of R_{dark}^{25} vs leaf N
409 and LMA did not significantly improve the relationships. For leaf A^{25}, correlations with LMA
410 and N either independently or combined were stronger on an area basis than on a mass basis.

411 Whereas for $R_{dark\_}CO_2^{25}$ and $R_{dark\_}O_2^{25}$ there was no clear difference between area- and mass-
412 based relationships (Table S11).

413 *Grain yield at harvest and links with leaf traits at anthesis*

414 Grain yield varied (P<0.001) with TOS for Experiment I, being 5.1, 5.3 and 4.8 t ha^{-1} for TOS1,
415 TOS2 and TOS3, respectively, but not for 2018 (P=0.102) with yields of 2.4 (TOS1), 2.5
416 (TOS2) and 2.6 t ha^{-1} (TOS3). The relative change in yield for 2017 (range of -24 to +36%)
417 was less than that of 2018 (-25 to +105%). Ranking of genotypes based on their relative change
418 in mean yields from TOS1 for both TOS2 and TOS3 were similar for 2017 and 2018 (Fig. 6).
419 Spearman's Rank correlations of the relative change in yield were 0.84 (P<0.001) for 2017 and
420 0.93 (P<0.001) for 2018. Changes in individual leaf traits did not correlate with changes in
421 yield in response to growth under warmer conditions in 2017 or 2018 (Fig. S4).

Discussion

We used time of sowing (TOS) as a proxy for generating different thermal environments for field-grown wheat (Table 1 and S1), and tested if responses of temperature-normalized values of photosynthetic CO_2 uptake (A^{25} and $V_{cmax}{}^{25}$) and leaf dark respiration – measured as both CO_2 release and O_2 uptake (R_{dark}) – were consistent with generalized patterns of thermal acclimation. We observed that for the CO_2-exchange traits, warming (i.e. later dates of TOS) did not result in our hypothesized decreases in flag leaf A^{25}, $V_{cmax}{}^{25}$ or $R_{dark}{}^{25}$ (Fig. 1). Rather, these traits increased and/or remained unchanged response to warming with later sowing. The only exception was the reduced A^{25} at later TOS in 2018; however, in that case, the reduction in A^{25} was not due to a direct effect of warming on photosynthetic metabolism, but rather was a consequence of reduced stomatal conductance (with TOS 2 and 3 stomatal conductance being 56 and 33% less than that of TOS1, respectively) reflecting limitations in water availability during the few days of measurements in 2018 (Supplementary Table S3). Differences in the temperature sensitivities of the three CO_2 exchange traits meant that the balance between $R_{dark\_}CO_2{}^{25}$ and A^{25} or $V_{cmax}{}^{25}$ was altered by warming, with consistently lower $R_{dark\_}CO_2{}^{25}$:A^{25} and $R_{dark\_}CO_2{}^{25}$:$V_{cmax}{}^{25}$ at the warmest TOS relative to the earlier, cooler TOS (Table 3). Importantly, in contrast to the results for $R_{dark\_}CO_2{}^{25}$, O_2-based measures of leaf R_{dark} were lower at TOS2/3 compared with TOS1 (Fig. 2 and 3) - a result that supported our hypothesis that acclimation to warming is characterised by a downward shift in the R_{dark}-temperature response curve. The divergent temperature responses of CO_2- and O_2-based R_{dark} suggests different substrates drive respiratory processes in leaves of warmer-grown plants, as changes in the ratio of CO_2 efflux to O_2 uptake (i.e. respiratory quotient, RQ) are known to occur in response to shifts in the type of substrates used by respiratory metabolism (Dieuaide-Noubhani, Canioni, & Raymond, 1997; Lambers, Robinson, & Ribas-Carbo, 2005). Interestingly, there

were only weak, albeit significant, relationships between the leaf gas exchange and chemical/structural traits, with these relationships being unaffected by warming (Fig. S1-S3). We have previously reported similar weak relationships of $R_{dark\_O_2}$ with LMA, N_{area} and N_{mass} in wheat leaves across multiple genotypes from both glasshouse and field experiments (Coast et al., 2019). The weak R_{dark}-N relationships indicates that rates of R_{dark} are not contingent on increases in N concentration *per se* (Atkinson, Hellicar, Fitter, & Atkin, 2007) or are necessarily directly linked with rates of protein turnover. The varied TOS responses of wheat flag leaf gas exchange at anthesis were not reflective of overall crop performance, in terms of yield at harvest maturity (Fig. S4).

The use of TOS to investigate wheat responses to high growth temperature was probably confounded by changes in other environmental variables. We note that: (1) agronomic traits (days to flowering and plant height at harvest) were influenced by TOS (data not shown); (2) that such traits could have been due to not just temperature but also differences in photoperiod, input of solar radiation and soil temperature; and (3) that such trait differences could influence leaf and whole plant carbon dynamics.

Carbon-based leaf physiological processes did not acclimate to warming

Our results did not support our working hypothesis that acclimation of leaf CO_2 exchange traits, measured at a common temperature of 25°C (i.e. A^{25}, $V_{cmax}{}^{25}$ and $R_{dark\_}CO_2{}^{25}$), would be lower in leaves experiencing higher growth temperatures (i.e. TOS2/3) than in leaves developed under cooler conditions (i.e. TOS 1; Fig. 1). In support of this finding, leaf CO_2 exchange also did not acclimate to night-time warming in field-grown wheat (Impa et al., 2019). By contrast, previous studies have reported lower rates of temperature-normalized CO_2 exchange in warm vs cold acclimated plants across a range of species (Atkin & Tjoelker, 2003; Berry &

469 Bjorkman, 1980; Way & Yamori, 2014), but, more widely, the leaf physiology responses of
470 crop plants to elevated temperatures in field experiments have been inconsistent (Cai et al.,
471 2020; Cai et al., 2018; Zheng et al., 2018; Zhou et al., 2018), suggesting that crops do not
472 always exhibit classical thermal acclimation responses in the field. While the reason(s) for the
473 disparity in acclimation responses of crop plants is unclear, it is likely that differences in the
474 warming techniques, degree and duration of warming used in the field might be factors. For
475 example, in experiments where warming is imposed by heating only the air around leaves or
476 the crop canopy [e.g. by infrared radiators or with T-FACE (temperature with free-air CO_2
477 enrichment)], warming is restricted to the above-ground part of the plant, not the whole plant.
478 By contrast, when varying TOS, both air and soil temperature increase simultaneously, likely
479 promoting changes in growth and carbon demand of above- and below-ground tissues.
480 Moreover, use of TOS as a warming treatment introduces other variables (e.g. different day
481 lengths and input of solar radiation) that may, in themselves, influence rates of leaf gas
482 exchange, reduce the period of vegetative development and affect source activities. Seasonal
483 changes in day length can influence the temperature responses of leaf biochemical processes
484 (Stinziano, Way, & Bauerle, 2018; Yamaguchi, Nakaji, Hiura, & Hikosaka, 2016). Thus, there
485 is a need to disentangle the effect of temperature from changes in day length and solar radiation.

486 Why were temperature-normalized rates of CO_2 exchange higher in TOS2/3 plants
487 compared to their TOS1 counterparts (Fig. 1, Table 2)? Later sowing is associated with warmer
488 days and longer photoperiods – conditions that increase the rate of development of sink tissues
489 (i.e. meristematic regions of shoots and roots) in wheat canopies (Angus, Mackenzie, Morton,
490 & Schafer, 1981; Baker & Gallagher, 1983; Slafer & Rawson, 1996). This increase in sink
491 tissue development could increase the demand for photosynthetically fixed carbon from source
492 leaves creating a positive feedback effect on A^{25} and $V_{cmax}{}^{25}$ (Asao & Ryan, 2015; King,

493 Wardlaw, & Evans, 1967; Pinkard, Eyles, & O'Grady, 2011). Faster developmental rates in
494 sink tissues would also increase demand for respiratory products (e.g. ATP, NADH and carbon
495 skeletons) in source leaves – products needed to fuel higher rates of amino acid and sucrose
496 synthesis/export (Bouma, De Visser, Van Leeuwen, De Kock, & Lambers, 1995; Edwards,
497 Roberts, & Atwell, 2012; Li et al., 2017). Increased photosynthetic capacity (as indicated by
498 higher V_{cmax}^{25}) could also increase the demand for respiratory ATP needed to support processes
499 such as protein turnover and maintenance of ion gradients in source leaves (Atkin et al., 2017;
500 Fatichi, Leuzinger, & Körner, 2014; Lambers et al., 2005). Together, such factors – which point
501 to a tight coupling of metabolism in source and sink tissues of field grown wheat - may explain
502 why rates of CO_2 exchange were higher at TOS2/3 than at TOS1.

503 Along with the finding that rates of CO_2 exchange increased with increasing TOS, we
504 observed a positive relationship of leaf photosynthetic capacity and $R_{dark\_}CO_2$ with the recent
505 T_{min} and T_{max} values experienced by plants at anthesis (Fig. 4). Global observed trends and
506 model projections show greater increases in land surface T_{min} than T_{max} (Vose, Easterling, &
507 Gleason, 2005), with the increase in T_{min} being more strongly related to global yield decline of
508 major crops than increases in T_{max} (García, Dreccer, Miralles, & Serrago, 2015; García,
509 Serrago, Dreccer, & Miralles, 2016; Peng et al., 2004). The T_{min} during anthesis may act to
510 stimulate leaf $R_{dark\_}CO_2$ by altering biosynthetic processes such as rates of protein turnover and
511 costs associated with sucrose export, increasing carbon loss in source leaves and reducing
512 carbohydrate translocation from leaves to sink organs, with negative effects on plant growth
513 and yield (Sadok & Jagadish, 2020). A recent analysis of metabolite profiles of leaves of wheat
514 exposed to high T_{min} showed increased concentrations of tricarboxylic acid cycle related
515 metabolites, which support increased rates of leaf $R_{dark\_}CO_2$ (Impa et al., 2019).

516 *The balance of $R_{dark}\_CO_2^{25}$ to A^{25} or V_{cmax}^{25} was reduced by warming*

517 The processes of carbon release by leaf respiration and carbon uptake by photosynthesis are
518 often correlated (Loveys et al., 2003; Reich et al., 1998; Whitehead et al., 2004). This reflects
519 a physiological interdependence of the two processes (Hurry et al., 2005; Kromer, 1995; Way
520 & Yamori, 2014), such as the dependence of respiratory metabolism on photosynthesis for
521 substrates, the demands for ATP associated with exporting assimilates, and the need for
522 respiration-generated energy to maintain photosynthetic activity including sucrose synthesis
523 and transport or phloem loading (Bouma et al., 1995). Based on these observations, several
524 studies have assumed that the temperature-normalized ratios of $R_{\text{dark}}\_CO_2$ to A, and by
525 extension V_{cmax}, should be constant among plants experiencing a range of different growth
526 temperatures. This assumption is incorporated in some Earth System modelling frameworks
527 such as MOSES-TRIFFID (now JULES), CLM and Century (Cox, 2001; Melillo et al., 1993;
528 Oleson et al., 2013). However, temperature-normalized values of leaf $R_{\text{dark}}\_CO_2$, A and V_{cmax}
529 may not acclimate to sustained warming to the same degree. These differences would alter the
530 balance between $R_{\text{dark}}\_CO_2^{25}$ and A^{25} ($R_{\text{dark}}\_CO_2^{25}$:$A^{25}$) or $R_{\text{dark}}\_CO_2^{25}$ and V_{cmax}
531 ($R_{\text{dark}}\_CO_2^{25}$:$V_{\text{cmax}}^{25}$). In our study, the range of $R_{\text{dark}}\_CO_2^{25}$:$V_{\text{cmax}}^{25}$ for TOS1 was 0.012–0.015,
532 values that are consistent with the assumed $R_{\text{dark}}\_CO_2^{25}$:$V_{\text{cmax}}^{25}$ value (0.015) used in JULES
533 and other ESM, but considerably lower than the mean for C_3 herbs/grasses (0.078) reported for
534 plants growing in natural ecosystems across the globe (Atkin et al., 2015). Our findings that
535 $R_{\text{dark}}\_CO_2^{25}$:$A^{25}$ and $R_{\text{dark}}\_CO_2^{25}$:$V_{\text{cmax}}^{25}$ were lower in the warmest thermal regime (i.e. TOS3;
536 Table 3) are, however, in agreement with the global pattern (Atkin et al., 2015) and that
537 observed in cucumber and tomato (Ikkonen, Shibaeva, & Titov, 2018). Moreover, our results
538 showed $R_{\text{dark}}\_CO_2^{25}$:$A^{25}$ increasing in leaves experiencing water-deficit (as shown by the higher
539 $R_{\text{dark}}\_CO_2^{25}$:$A^{25}$ ratios in plants that had low stomatal conductance in 2018, Table 3), yet

$R_{dark}\_CO_2^{25}$:V_{cmax}^{25} was unchanged under these conditions. This suggests that variations in leaf respiration are more closely tied to variations in Rubisco capacity, rather than to the limits of net photosynthesis.

Oxygen based measure of leaf respiration acclimated to warming

In contrast to the growing number of studies that have investigated acclimation of $R_{dark}\_CO_2$ to warming by a range of field-grown plants in natural and managed environments, studies on acclimation of $R_{dark}\_O_2$ to warming by field-grown plants – including crops - have been limited. This is probably because techniques for measuring leaf $R_{dark}\_O_2$ are generally cumbersome and low throughput. To overcome this, we used a high-throughput technique described by Scafaro et al. (2017) – and used for wheat (Coast et al., 2019), *Arabidopsis thaliana* (O'Leary et al., 2017) and *Eucalyptus camaldulensis* (Asao et al., 2020) - to measure wheat flag leaf $R_{dark}\_O_2$ at four temperatures over the 20-35°C range. In addition to allowing comparisons of temperature-normalized (i.e. at 25°C) rates of $R_{dark}\_O_2$, this enabled us to test whether the slope and elevation of the short-term response of leaf $R_{dark}\_O_2$ in 20 wheat genotypes was affected by growth environment in two experiments. The results showed that wheat flag leaf $R_{dark}\_O_2$ decreased with increasing growth temperature (Fig. 2) – a result that contrasted with the responses of $R_{dark}\_CO_2^{25}$ (see above and Fig. 1). The leaf $R_{dark}\_O_2$ response in our study is consistent with expectations for $R_{dark}\_O_2$ (see reviews by Atkin & Tjoelker, 2003; Slot & Kitajima, 2015) and earlier observations on how rates of CO_2-based leaf R_{dark} of tree species respond to warming under field settings (Drake et al., 2015; Reich et al., 2016). In both experiments within our study, flag leaves which developed under the warmer conditions of TOS2 and TOS3 generally exhibited lower rates of leaf $R_{dark}\_O_2$ across a range of measuring temperatures (i.e. Type II acclimation; Atkin and Tjoelker, 2003), with the exception being

563 TOS3 of 2018 where Type I acclimation (i.e. warm-grown plants exhibit a lower Q_{10} value
564 than their cold-grown counterparts; Atkin and Tjoelker, 2003) was observed (Fig. 3). Type II
565 acclimation is the more common type of acclimation for leaves that develop under warmer
566 conditions (Slot & Kitajima, 2015), and is likely the result of changes in mitochondrial number,
567 structure and/or protein composition (Atkin, Bruhn, & Tjoelker, 2005). On the other hand, with
568 Type I acclimation (i.e. declining Q_{10}), the reduction in $R_{dark\_}O_2$ at high measuring temperatures
569 is likely due to underlying factors regulating respiratory flux, including depletion of available
570 substrate and/or reduction in turnover of ATP to ADP (Atkin & Tjoelker, 2003). On average,
571 the Q_{10} (the short-term temperature response) of $R_{dark\_}O_2$ at TOS1 in both experiments were
572 close to the mean reported for crops including field beans and wheat (2.3; Larigauderie &
573 Körner, 1995) – being 2.0 and 2.4 in 2017 and 2018, respectively.

574 *The varied temperature responses of CO_2 and O_2 based leaf respiration suggests switch in*
575 *respiratory substrates*

576 As noted above, differences in the growth temperature responses of $R_{dark\_}CO_2$ (no acclimation,
577 increasing with warming; Fig. 1) and $R_{dark\_}O_2$ (acclimation, decreasing with warming; Fig. 2
578 and 3) suggest changes in the substrate used by respiration. In plants, the main respiratory
579 substrates are soluble carbohydrates (Plaxton & Podestá, 2006), with oxidation of glucose
580 resulting in a respiratory quotient (RQ, the molar ratio of CO_2 produced per O_2 consumed
581 during R_{dark}) of 1.0. Under stress and conditions that reduce rates of photosynthetic fixation of
582 carbon, the source of respiratory substrate can shift from carbohydrates to other stored organic
583 compounds (Araújo, Tohge, Ishizaki, Leaver, & Fernie, 2011). We observed consistent
584 increases in RQ with warming (when comparing late vs early TOS) in both experiments.
585 Increases in RQ point to a switch to more oxidised substrates such as organic acids. Further

work is needed to investigate the nature of the respiratory substrate used during warming in crops. This would involve concurrent measurements of gas exchange (O_2 and CO_2 fluxes, which is difficult) and complementary estimates of respiratory substrate pool sizes. However, current techniques for such measurements are cumbersome (e.g. membrane inlet mass spectrometers and the cavity-enhanced Raman multi-gas spectrometry (Keiner, Frosch, Massad, Trumbore, & Popp, 2014), limiting their application in large-scale field studies.

In conclusion, our study has shown that the response of leaf gas exchange to warming is not fixed in field-grown wheat. The oxygen-based measurement of leaf respiration, $R_{dark\_}O_2$, acclimated to warming. By contrast, the CO_2-based measure of R_{dark}, $R_{dark\_}CO_2$, did not acclimate but instead increased with TOS/warming, suggesting that the substrates used by leaf respiration changed with TOS/warming. These varied physiological responses to warming have implications for crop models that assume a fixed temperature response of leaf physiological processes.

599 **Acknowledgements**

600 The authors have no conflicts of interest to declare. The authors are grateful for the support of
601 the ARC Centre of Excellence in Plant Energy Biology (CE140100008), and the Grains
602 Research and Development Corporation National Wheat Heat Tolerance Project US00080. We
603 thank Claire Brown and Amy Smith of Birchip Cropping Group, Victoria for managing field
604 trials in Victoria and Sabina Yasmin of The University of Sydney Plant Breeding Institute,
605 Narrabri for data management. We are also grateful to the farmers who generously provided
606 us with field sites for 2017 and 2018.

607 **References**

608 Angus, J. F., Mackenzie, D. H., Morton, R., & Schafer, C. A. (1981). Phasic development in
609 field crops II. Thermal and photoperiodic responses of spring wheat. *Field Crops*
610 *Research, 4*, 269-283. doi:https://doi.org/10.1016/0378-4290(81)90078-2

611 Anna, F. A., Logan, D. C., & Atkin, O. K. (2006). On the developmental dependence of leaf
612 respiration: responses to short- and long-term changes in growth temperature. *American*
613 *Journal of Botany, 93*(11), 1633-1639.

614 Araújo, W. L., Tohge, T., Ishizaki, K., Leaver, C. J., & Fernie, A. R. (2011). Protein
615 degradation–an alternative respiratory substrate for stressed plants. *Trends in Plant*
616 *Science, 16*(9), 489-498.

617 Asao, S., Hayes, L., Aspinwall, M. J., Rymer, P. D., Blackman, C., Bryant, C. J., . . . Atkin, O.
618 K. (2020). Leaf trait variation is similar among genotypes of *Eucalyptus camaldulensis*
619 from differing climates and arises as plastic response to season rather than water
620 availability. *New Phytologist, 227*(3),780-793. doi:10.1111/nph.16579

621 Asao, S., & Ryan, M. G. (2015). Carbohydrate regulation of photosynthesis and respiration
622 from branch girdling in four species of wet tropical rain forest trees. *Tree Physiology,*
623 *35*(6), 608-620.

624 Asseng, S., Ewert, F., Rosenzweig, C., Jones, J. W., Hatfield, J. L., Ruane, A. C., . . .
625 Cammarano, D. (2013). Uncertainty in simulating wheat yields under climate change.
626 *Nature Climate Change, 3*(9), 827-832.

627 Athanasiou, K., Dyson, B. C., Webster, R. E., & Johnson, G. N. (2010). Dynamic acclimation
628 of photosynthesis increases plant fitness in changing environments. *Plant Physiology,*
629 *152*(1), 366-373. doi:10.1104/pp.109.149351

630 Atkin, O., Bruhn, D., & Tjoelker, M. (2005). Response of plant respiration to changes in
631 temperature: mechanisms and consequences of variations in Q_{10} values and
632 acclimation. In *Plant Respiration*: *Vol. 18* (pp. 95-135). Springer, Dordrecht, The
633 Netherlands: Springer.
634 Atkin, O. K., Bahar, N. H. A., Bloomfield, K. J., Griffin, K. L., Heskel, M. A., Huntingford,
635 C., . . . Turnbull, M. H. (2017). Leaf respiration in terrestrial biosphere models. In G.
636 Tcherkez & J. Ghashghaie (Eds.), *Plant Respiration: Metabolic Fluxes and Carbon*
637 *Balance* (pp. 109-145). Cham, Switzerland: Springer Nature.
638 Atkin, O. K., Bloomfield, K. J., Reich, P. B., Tjoelker, M. G., Asner, G. P., Bonal, D., . . .
639 Zaragoza-Castells, J. (2015). Global variability in leaf respiration in relation to climate,
640 plant functional types and leaf traits. *New Phytologist, 206*(2), 614-636.
641 doi:10.1111/nph.13253
642 Atkin, O. K., Evans, J. R., & Siebke, K. (1998). Relationship between the inhibition of leaf
643 respiration by light and enhancement of leaf dark respiration following light treatment.
644 *Australian Journal of Plant Physiology, 25*. doi:10.1071/PP97159
645 Atkin, O. K., & Tjoelker, M. G. (2003). Thermal acclimation and the dynamic response of
646 plant respiration to temperature. *Trends in Plant Science, 8*(7), 343-351.
647 doi:10.1016/S1360-1385(03)00136-5
648 Atkinson, L. J., Hellicar, M. A., Fitter, A. H., & Atkin, O. K. (2007). Impact of temperature on
649 the relationship between respiration and nitrogen concentration in roots: an analysis of
650 scaling relationships, Q_{10} values and thermal acclimation ratios. *New Phytologist,*
651 *173*(1), 110-120.

652 Azcon-Bieto, J., Day, D. A., & Lambers, H. (1983). The regulation of respiration in the dark
653 in wheat leaf slices. *Plant Science Letters, 32*(3), 313-320. doi:10.1016/0304-
654 4211(83)90037-8
655 Badger, M. R., & Collatz, G. J. (1977). Studies on the kinetic mechanism of ribulose-1, 5-
656 bisphosphate carboxylase and oxygenase reactions, with particular reference to the
657 effect of temperature on kinetic parameters. *Carnegie Institute of Washington*
658 *Yearbook, 76*, 355-361.
659 Baker, C. K., & Gallagher, J. N. (1983). The development of winter wheat in the field. 2. The
660 control of primordium initiation rate by temperature and photoperiod. *The Journal of*
661 *Agricultural Science, 101*(2), 337-344. doi:10.1017/S0021859600037643
662 Bassu, S., Brisson, N., Durand, J.-L., Boote, K., Lizaso, J., Jones, J. W., . . . Waha, K. (2014).
663 How do various maize crop models vary in their responses to climate change factors?
664 *Global Change Biology, 20*(7), 2301-2320. doi:10.1111/gcb.12520
665 Berry, J., & Bjorkman, O. (1980). Photosynthetic response and adaptation to temperature in
666 higher-plants. *Annual Review of Plant Physiology and Plant Molecular Biology, 31*,
667 491-543. doi:DOI 10.1146/annurev.pp.31.060180.002423
668 Bouma, T., De Visser, R., Van Leeuwen, P., De Kock, M., & Lambers, H. (1995). The
669 respiratory energy requirements involved in nocturnal carbohydrate export from starch-
670 storing mature source leaves and their contribution to leaf dark respiration. *Journal of*
671 *Experimental Botany, 46*(9), 1185-1194.
672 Cai, C., Li, G., Di, L., Ding, Y., Fu, L., Guo, X., . . . Yin, X. (2020). The acclimation of leaf
673 photosynthesis of wheat and rice to seasonal temperature changes in T-FACE
674 environments. *Global Change Biology, 26*(2), 539-556. doi:10.1111/gcb.14830

675 Cai, C., Li, G., Yang, H., Yang, J., Liu, H., Struik, P. C., . . . Zhu, J. (2018). Do all leaf
676 photosynthesis parameters of rice acclimate to elevated CO_2, elevated temperature, and
677 their combination, in FACE environments? *Global Change Biology, 24*(4), 1685-1707.
678 doi:10.1111/gcb.13961
679 Campbell, C., Atkinson, L., Zaragoza-Castells, J., Lundmark, M., Atkin, O., & Hurry, V.
680 (2007). Acclimation of photosynthesis and respiration is asynchronous in response to
681 changes in temperature regardless of plant functional group. *New Phytologist, 176*(2),
682 375-389.
683 Coast, O., Shah, S., Ivakov, A., Gaju, O., Wilson, P. B., Posch, B. C., . . . Atkin, O. K. (2019).
684 Predicting dark respiration rates of wheat leaves from hyperspectral reflectance. *Plant,*
685 *Cell & Environment*, *42*(7), 2133-2150. doi:doi:10.1111/pce.13544
686 Collins, M., Knutti, R., Arblaster, J., Dufresne, J.-L., Fichefet, T., Friedlingstein, P., . . .
687 Krinner, G. (2013). Long-term climate change: projections, commitments and
688 irreversibility. In *Climate Change 2013-The Physical Science Basis: Contribution of*
689 *Working Group I to the Fifth Assessment Report of the Intergovernmental Panel on*
690 *Climate Change* (pp. 1029-1136): Cambridge University Press.
691 Cox, P. (2001). *Description of the "TRIFFID" dynamic global vegetation model.* Bracknell:
692 Hadley Centre, Met Office.
693 Crafts-Brandner, S. J., & Salvucci, M. E. (2002). Sensitivity of photosynthesis in a C_4 plant,
694 maize, to heat stress. *Plant Physiology, 129*(4), 1773-1780.
695 De Kauwe, M. G., Lin, Y.-S., Wright, I. J., Medlyn, B. E., Crous, K. Y., Ellsworth, D. S., . . .
696 Domingues, T. F. (2016). A test of the 'one-point method' for estimating maximum
697 carboxylation capacity from field-measured, light-saturated photosynthesis. *New*
698 *Phytologist, 210*(3), 1130-1144.

699 Dieuaide-Noubhani, M., Canioni, P., & Raymond, P. (1997). Sugar-starvation-induced
700 changes of carbon metabolism in excised maize root tips. *Plant Physiology, 115*(4),
701 1505-1513. doi:10.1104/pp.115.4.1505
702 Donatelli, M., Srivastava, A. K., Duveiller, G., Niemeyer, S., & Fumagalli, D. (2015). Climate
703 change impact and potential adaptation strategies under alternate realizations of climate
704 scenarios for three major crops in Europe. *Environmental Research Letters, 10*(7),
705 075005. doi:10.1088/1748-9326/10/7/075005
706 Drake, J. E., Aspinwall, M. J., Pfautsch, S., Rymer, P. D., Reich, P. B., Smith, R. A., . . .
707 Tjoelker, M. G. (2015). The capacity to cope with climate warming declines from
708 temperate to tropical latitudes in two widely distributed Eucalyptus species. *Global*
709 *Change Biology, 21*(1), 459-472.
710 Edwards, J. M., Roberts, T. H., & Atwell, B. J. (2012). Quantifying ATP turnover in anoxic
711 coleoptiles of rice (*Oryza sativa*) demonstrates preferential allocation of energy to
712 protein synthesis. *Journal of Experimental Botany, 63*(12), 4389-4402.
713 Evans, J. R., Voncaemmerer, S., Setchell, B. A., & Hudson, G. S. (1994). The relationship
714 between CO_2 transfer conductance and leaf anatomy in transgenic tobacco with a
715 reduced content of rubisco. *Australian Journal of Plant Physiology, 21*(4), 475-495.
716 doi:Doi 10.1071/Pp9940475
717 Fatichi, S., Leuzinger, S., & Körner, C. (2014). Moving beyond photosynthesis: from carbon
718 source to sink-driven vegetation modeling. *New Phytologist, 201*(4), 1086-1095.
719 Doi:10.1111/nph.12614
720 Frenkel, M., Bellafiore, S., Rochaix, J.-D., & Jansson, S. (2007). Hierarchy amongst
721 photosynthetic acclimation responses for plant fitness. *Physiologia Plantarum, 129*(2),
722 455-459. Doi:10.1111/j.1399-3054.2006.00831.x

García, G. A., Dreccer, M. F., Miralles, D. J., & Serrago, R. A. (2015). High night temperatures during grain number determination reduce wheat and barley grain yield: a field study. *Global Change Biology, 21*(11), 4153-4164. Doi:10.1111/gcb.13009

García, G. A., Serrago, R. A., Dreccer, M. F., & Miralles, D. J. (2016). Post-anthesis warm nights reduce grain weight in field-grown wheat and barley. *Field Crops Research, 195*, 50-59. Doi:10.1016/j.fcr.2016.06.002

Ghannoum, O., Phillips, N. G., Sears, M. A., Logan, B. A., Lewis, J. D., Conroy, J. P., & Tissue, D. T. (2010). Photosynthetic responses of two eucalypts to industrial-age changes in atmospheric [CO_2] and temperature. *Plant, Cell & Environment, 33*(10), 1671-1681. Doi:10.1111/j.1365-3040.2010.02172.x

Hansen, S., Jensen, H., Nielsen, N., & Svendsen, H. (1991). Simulation of nitrogen dynamics and biomass production in winter wheat using the Danish simulation model DAISY. *Fertilizer Research, 27*(2-3), 245-259.

Haxeltine, A., & Prentice, I. C. (1996). BIOME3: An equilibrium terrestrial biosphere model based on ecophysiological constraints, resource availability, and competition among plant functional types. *Global Biogeochemical Cycles, 10*(4), 693-709.

Hikosaka, K., Ishikawa, K., Borjigidai, A., Muller, O., & Onoda, Y. (2006). Temperature acclimation of photosynthesis: mechanisms involved in the changes in temperature dependence of photosynthetic rate. *Journal of Experimental Botany*, *57*(2), 291-302.

Hochman, Z., Gobbett, D. L., & Horan, H. (2017). Climate trends account for stalled wheat yields in Australia since 1990. *Global Change Biology, 23*(5), 2071-2081. Doi:10.1111/gcb.13604

745 Hunt, J. R., Lilley, J. M., Trevaskis, B., Flohr, B. M., Peake, A., Fletcher, A., . . . Kirkegaard,
746 J. A. (2019). Early sowing systems can boost Australian wheat yields despite recent
747 climate change. *Nature Climate Change, 9*(3), 244.
748 Huntingford, C., Atkin, O. K., Martinez-de la Torre, A., Mercado, L. M., Heskel, M. A.,
749 Harper, A. B., . . . Malhi, Y. (2017). Implications of improved representations of plant
750 respiration in a changing climate. *Nature Communications, 8*(1), 1602.
751 Doi:10.1038/s41467-017-01774-z
752 Hurry, V., Igamberdiev, A., Keerberg, O., Pärnik, T., Atkin, O., Zaragoza-Castells, J., &
753 Gardeström, P. (2005). Respiration in photosynthetic cells: gas exchange components,
754 interactions with photorespiration and the operation of mitochondria in the light. In,
755 *Plant Respiration: Vol. 18* (pp. 43-61). Dordrecht, The Netherlands: Springer.
756 Ikkonen, E. N., Shibaeva, T. G., & Titov, A. F. (2018). Influence of daily short-term
757 temperature drops on respiration to photosynthesis ratio in chilling-sensitive plants.
758 *Russian Journal of Plant Physiology, 65*(1), 78-83. Doi:10.1134/s1021443718010041
759 Impa, S. M., Sunoj, V. S. J., Krassovskaya, I., Bheemanahalli, R., Obata, T., & Jagadish, S. V.
760 K. (2019). Carbon balance and source-sink metabolic changes in winter wheat exposed
761 to high night-time temperature. *Plant, Cell & Environment, 42*(4), 1233-1246.
762 Doi:10.1111/pce.13488
763 Isbell, R. F. (1996). *The Australian Soil Classification*. Melbourne, Australia: CSIRO
764 Publishing.
765 Keiner, R., Frosch, T., Massad, T., Trumbore, S., & Popp, J. (2014). Enhanced Raman multigas
766 sensing–a novel tool for control and analysis of $^{13}CO_2$ labeling experiments in
767 environmental research. *Analyst, 139*(16), 3879-3884.

King, R. W., Wardlaw, I. F., & Evans, L. T. (1967). Effect of assimilate utilization on photosynthetic rate in wheat. *Planta, 77*(3), 261-276. Doi:10.1007/BF00385296

Kirkegaard, J. A., Lilley, J. M., Brill, R. D., Sprague, S. J., Fettell, N. A., & Pengilley, G. C. (2016). Re-evaluating sowing time of spring canola (*Brassica napus* L.) in South-Eastern Australia—how early is too early? *Crop and Pasture Science, 67*(3–4), 381-396, 316.

Knorr, W. (2000). Annual and interannual CO_2 exchanges of the terrestrial biosphere: process-based simulations and uncertainties. *Global Ecology and Biogeography, 9*(3), 225-252. Doi:10.1046/j.1365-2699.2000.00159.x

Kromer, S. (1995). Respiration during photosynthesis. *Annual Review of Plant Biology, 46*(1), 45-70.

Lambers, H., Robinson, S. A., & Ribas-Carbo, M. (2005) Regulation of respiration *in vivo*. In, *Advances in Photosynthesis and Respiration Series: Vol. 18* (pp. 1-15). Dordrecht, The Netherlands: Springer.

Larigauderie, A., & Körner, C. (1995). Acclimation of leaf dark respiration to temperature in alpine and lowland plant species. *Annals of Botany, 76*(3), 245-252.

Li, L., Nelson, C. J., Trösch, J., Castleden, I., Huang, S., & Millar, A. H. (2017). Protein degradation rate in *Arabidopsis thaliana* leaf growth and development. *The Plant Cell, 29*(2), 207-228.

Li, T., Hasegawa, T., Yin, X., Zhu, Y., Boote, K., Adam, M., . . . Bouman, B. (2015). Uncertainties in predicting rice yield by current crop models under a wide range of climatic conditions. *Global Change Biology, 21*(3), 1328-1341. Doi:10.1111/gcb.12758

791 Lin, Y.-S., Medlyn, B. E., & Ellsworth, D. S. (2012). Temperature responses of leaf net
792 photosynthesis: the role of component processes. *Tree Physiology, 32*(2), 219-231.
793 Liu, B., Asseng, S., Müller, C., Ewert, F., Elliott, J., Lobell, David B., . . . Zhu, Y. (2016).
794 Similar estimates of temperature impacts on global wheat yield by three independent
795 methods. *Nature Climate Change, 6*, 1130. Doi:10.1038/nclimate3115
796 Lobell, D. B., & Gourdji, S. M. (2012). The influence of climate change on global crop
797 productivity. *Plant Physiology, 160*(4), 1686-1697. Doi:10.1104/pp.112.208298
798 Loveys, B. R., Atkinson, L. J., Sherlock, D. J., Roberts, R. L., Fitter, A. H., & Atkin, O. K.
799 (2003). Thermal acclimation of leaf and root respiration: an investigation comparing
800 inherently fast- and slow-growing plant species. *Global Change Biology, 9*(6), 895-
801 910. Doi:DOI 10.1046/j.1365-2486.2003.00611.x
802 Melillo, J. M., McGuire, A. D., Kicklighter, D. W., Moore, B., Vorosmarty, C. J., & Schloss,
803 A. L. (1993). Global climate change and terrestrial net primary production. *Nature,*
804 *363*(6426), 234-240. Doi:10.1038/363234a0
805 O'Leary, B. M., Lee, C. P., Atkin, O. K., Cheng, R. Y., Brown, T. B., & Millar, A. H. (2017).
806 Variation in leaf respiration rates at night correlates with carbohydrate and amino acid
807 supply. *Plant Physiology, 174*(4), 2261-2273. doi:10.1104/pp.17.00610
808 O'Sullivan, O. S., Weerasinghe, K. W. L. K., Evans, J. R., Egerton, J. J. G., Tjoelker, M. G., &
809 Atkin, O. K. (2013). High-resolution temperature responses of leaf respiration in snow
810 gum (*Eucalyptus pauciflora*) reveal high-temperature limits to respiratory function.
811 *Plant, Cell & Environment, 36*(7), 1268-1284. doi:doi:10.1111/pce.12057
812 Oleson, K., Lawrence, D. M., Bonan, G. B., Drewniak, B., Huang, M., Koven, C. D., . . . Yang,
813 Z.-L. (2013). *Technical Description of version 4.5 of the Community Land Model*
814 *(CLM)* (NCAR/TN-503+STR). Boulder, CO:

Peng, S., Huang, J., Sheehy, J. E., Laza, R. C., Visperas, R. M., Zhong, X., . . . Cassman, K. G. (2004). Rice yields decline with higher night temperature from global warming. *Proceedings of the National Academy of Sciences, 101*(27), 9971-9975. doi:10.1073/pnas.0403720101

Pinkard, E. A., Eyles, A., & O'Grady, A. P. (2011). Are gas exchange responses to resource limitation and defoliation linked to source:sink relationships? *Plant, Cell & Environment, 34*(10), 1652-1665. doi:10.1111/j.1365-3040.2011.02361.x

Plaxton, W. C., & Podestá, F. E. (2006). The functional organization and control of plant respiration. *Critical Reviews in Plant Sciences, 25*(2), 159-198.

Rashid, F. A. A., Crisp, P. A., Zhang, Y., Berkowitz, O., Pogson, B. J., Day, D. A., . . . Scafaro, A. P. (2020). Molecular and physiological responses during thermal acclimation of leaf photosynthesis and respiration in rice. *Plant, Cell & Environment, 43*(3), 594-610. doi:10.1111/pce.13706

Reich, P. B., Ellsworth, D. S., & Walters, M. B. (1998). Leaf structure (specific leaf area) modulates photosynthesis–nitrogen relations: evidence from within and across species and functional groups. *Functional Ecology, 12*(6), 948-958.

Reich, P. B., Sendall, K. M., Stefanski, A., Wei, X., Rich, R. L., & Montgomery, R. A. (2016). Boreal and temperate trees show strong acclimation of respiration to warming. *Nature, 531*(7596), 633-636. doi:10.1038/nature17142

Reich, P. B., Tjoelker, M. G., Pregitzer, K. S., Wright, I. J., Oleksyn, J., & Machado, J. L. (2008). Scaling of respiration to nitrogen in leaves, stems and roots of higher land plants. *Ecology Letters, 11*(8), 793-801. doi:10.1111/j.1461-0248.2008.01185.x

Reich, P. B., Walters, M. B., Ellsworth, D. S., Vose, J. M., Volin, J. C., Gresham, C., & Bowman, W. D. (1998). Relationships of leaf dark respiration to leaf nitrogen, specific

839 leaf area and leaf life-span: a test across biomes and functional groups. *Oecologia, 114*(4), 471-482. doi:10.1007/s004420050471
841 Rosenzweig, C., Jones, J. W., Hatfield, J. L., Ruane, A. C., Boote, K. J., Thorburn, P., . . .
842 Winter, J. M. (2013). The Agricultural Model Intercomparison and Improvement
843 Project (AgMIP): Protocols and pilot studies. *Agricultural and Forest Meteorology, 170*, 166-182. doi:https://doi.org/10.1016/j.agrformet.2012.09.011
845 Ruan, Y. L., Patrick, J. W., Bouzayen, M., Osorio, S., & Fernie, A. R. (2012). Molecular
846 regulation of seed and fruit set. *Trends in Plant Science*, *17*(11), 656-665.
847 Ruimy, A., Dedieu, G., & Saugier, B. (1996). TURC: A diagnostic model of continental gross
848 primary productivity and net primary productivity. *Global Biogeochemical Cycles, 10*(2), 269-285.
850 Sadok, W., & Jagadish, K. (2020). The hidden costs of nighttime warming on yields. *Trends
851 in Plant Science*. *25*(7), 644-651. doi:10.1016/j.tplants.2020.02.003
852 Sage, R. F., & Kubien, D. S. (2007). The temperature response of C_3 and C_4 photosynthesis.
853 *Plant, Cell & Environment, 30*(9), 1086-1106.
854 Sage, R. F., & McKown, A. D. (2006). Is C_4 photosynthesis less phenotypically plastic than C_3
855 photosynthesis? *Journal of Experimental Botany*, *57*(2), 303-317.
856 Scafaro, A. P., Negrini, A. C. A., O'Leary, B., Rashid, F. A. A., Hayes, L., Fan, Y., . . . Atkin,
857 O. K. (2017). The combination of gas-phase fluorophore technology and automation to
858 enable high-throughput analysis of plant respiration. *Plant Methods, 13*(1), 16.
859 doi:10.1186/s13007-017-0169-3
860 Slafer, G. A., & Rawson, H. M. (1996). Responses to photoperiod change with phenophase
861 and temperature during wheat development. *Field Crops Research, 46*(1), 1-13.
862 doi:https://doi.org/10.1016/0378-4290(95)00081-X

Slot, M., & Winter, K. (2016). The Effects of Rising Temperature on the Ecophysiology of Tropical Forest Trees. *Tropical Tree Physiology: Adaptations and Responses in a Changing Environment.* G. Goldstein, G., & Santiago, L.S.. Cham, Springer International Publishing**:** 385-412.

Slot, M., & Kitajima, K. (2015). General patterns of acclimation of leaf respiration to elevated temperatures across biomes and plant types. *Oecologia, 177*(3), 885-900.

Smith, N. G., & Dukes, J. S. (2013). Plant respiration and photosynthesis in global-scale models: incorporating acclimation to temperature and CO_2. *Global Change Biology, 19*(1), 45-63. doi:doi:10.1111/j.1365-2486.2012.02797.x

Stinziano, J. R., Way, D. A., & Bauerle, W. L. (2018). Improving models of photosynthetic thermal acclimation: Which parameters are most important and how many should be modified? *Global Change Biology, 24*(4), 1580-1598. doi:10.1111/gcb.13924

Tjoelker, M. G., Oleksyn, J., Reich, P. B., & Żytkowiak, R. (2008). Coupling of respiration, nitrogen, and sugars underlies convergent temperature acclimation in Pinus banksiana across wide-ranging sites and populations. *Global Change Biology, 14*(4), 782-797.

Ullah, S., Bramley, H., Daetwyler, H., He, S., Mahmood, T., Thistlethwaite, R., & Trethowan, R. (2018). Genetic contribution of Emmer wheat (*Triticum dicoccon* Schrank) to heat tolerance of bread wheat. *Frontiers in Plant Science*, 9, 1529.

von Caemmerer, S., Evans, J. R., Hudson, G. S., & Andrews, T. J. (1994). The kinetics of ribulose-1,5-bisphosphate carboxylase/oxygenase *in vivo* inferred from measurements of photosynthesis in leaves of transgenic tobacco. *Planta, 195*(1), 88-97. doi:10.1007/bf00206296

885 Vose, R. S., Easterling, D. R., & Gleason, B. (2005). Maximum and minimum temperature
886 trends for the globe: An update through 2004. *Geophysical Research Letters, 32*(23).
887 doi:Artn L2382210.1029/2005gl024379
888 Wang, B., Feng, P., Chen, C., Li Liu, D., Waters, C., & Yu, Q. (2019). Designing wheat
889 ideotypes to cope with future changing climate in South-Eastern Australia. *Agricultural*
890 *Systems, 170*, 9-18.
891 Wang, E., Martre, P., Zhao, Z., Ewert, F., Maiorano, A., Rötter, R. P., . . . White, J. W. (2017).
892 The uncertainty of crop yield projections is reduced by improved temperature response
893 functions. *Nature Plants, 3*(8), 1-13.
894 Way, D. A., & Sage, R. F. (2008). Thermal acclimation of photosynthesis in black spruce
895 [*Picea mariana* (Mill.) BSP]. *Plant, Cell & Environment, 31*(9), 1250-1262.
896 Way, D. A., & Yamori, W. (2014). Thermal acclimation of photosynthesis: on the importance
897 of adjusting our definitions and accounting for thermal acclimation of respiration.
898 *Photosynthesis Research, 119*(1-2), 89-100. doi:10.1007/s11120-013-9873-7
899 Whitehead, D., Griffin, K. L., Turnbull, M. H., Tissue, D. T., Engel, V. C., Brown, K. J., . . .
900 Walcroft, A. S. (2004). Response of total night-time respiration to differences in total
901 daily photosynthesis for leaves in a *Quercus rubra* L. canopy: implications for
902 modelling canopy CO_2 exchange. *Global Change Biology, 10*(6), 925-938.
903 doi:10.1111/j.1365-2486.2004.00739.x
904 Wilson, K. B., Baldocchi, D. D., & Hanson, P. J. (2000). Spatial and seasonal variability of
905 photosynthetic parameters and their relationship to leaf nitrogen in a deciduous forest.
906 *Tree Physiology, 20*(9), 565-578.

907 Yamaguchi, D. P., Nakaji, T., Hiura, T., & Hikosaka, K. (2016). Effects of seasonal change
908 and experimental warming on the temperature dependence of photosynthesis in the
909 canopy leaves of Quercus serrata. *Tree Physiology, 36*(10), 1283-1295.
910 Zadoks, J. C., Chang, T. T., & Konzak, C. F. (1974). A decimal code for the growth stages of
911 cereals. *Weed Research, 14*(6), 415-421.
912 Zhao, Y. R., Li, X., Yu, K. Q., Cheng, F., & He, Y. (2016). Hyperspectral imaging for
913 determining pigment contents in cucumber leaves in response to angular leaf spot
914 disease. *Scientific Reports, 6*, 27790. doi:10.1038/srep27790
915 Zheng, Y. P., Li, R. Q., Guo, L. L., Hao, L. H., Zhou, H. R., Li, F., . . . Xu, M. (2018).
916 Temperature responses of photosynthesis and respiration of maize (*Zea mays*) plants to
917 experimental warming. *Russian Journal of Plant Physiology, 65*(4), 524-531.
918 doi:10.1134/s1021443718040192
919 Zhou, H., Xu, M., Hou, R., Zheng, Y., Chi, Y., & Ouyang, Z. (2018). Thermal acclimation of
920 photosynthesis to experimental warming is season dependent for winter wheat
921 (*Triticum aestivum* L.). *Environmental and Experimental Botany, 150*, 249-259.
922 doi:10.1016/j.envexpbot.2018.04.001
923 Ziehn, T., Kattge, J., Knorr, W., & Scholze, M. (2011). Improving the predictability of global
924 CO_2 assimilation rates under climate change. *Geophysical Research Letters, 38*(10).
925 doi:10.1029/2011gl047182

926 **Figure legends**

927 Figure 1. Mean rates of area-based net CO_2 assimilation rates at 25°C (A^{25}), maximum
928 carboxylation capacity of photosynthetic capacity (V_{cmax}^{25}), and leaf dark respiration at 25°C
929 taken as rate of CO_2 efflux ($R_{dark}\_CO_2^{25}$) for six selected wheat genotypes. Genotypes were
930 grown under three thermal regimes (by varying time of sowing, TOS) during 2017 (a, c and e)
931 and 2018 (b, d and f). Values are the mean of four plants (±standard error of mean).

932 Figure 2. Mean rates of leaf dark respiration on O_2 consumption basis at 25°C ($R_{dark}\_O_2^{25}$) for
933 six selected and the whole set of 20 wheat genotypes. Genotypes were grown under three
934 thermal regimes (by varying time of sowing, TOS) during 2017 (a, b) and 2018 (c, d). Values
935 are the mean of four plants (±standard error of mean).

936 Figure 3. Mean temperature response of leaf dark respiration (O_2 consumption; values shown
937 on a log scale) expressed per leaf area (R_{dark}) of 20 wheat genotypes grown under three thermal
938 regimes (by varying time of sowing, TOS) during 2017 (a) and 2018 (b). Values are the means
939 of four plants (±standard deviation) from each of 20 genotypes at the different TOS. Treatments
940 (or TOS) are significantly different (P<0.05) if the difference in their Q_{10} values is greater than
941 the indicated least significant difference (l.s.d.) value. Parameter estimates of the log-
942 transformed instantaneous leaf R_{dark}-temperature responses are given in Table S6.

943 Figure 4. Relationship of mean area-based leaf net CO_2 assimilation rate (A^{25}), maximum
944 carboxylation capacity of photosynthetic capacity (V_{cmax}^{25}) and rate of CO_2 efflux ($R_{dark}\_CO_2^{25}$)
945 at 25°C with average minimum temperature (open circles and solid lines) or maximum
946 temperature (open sqaures and dashed lines) of period before 50% of plants had achieved
947 anthesis (DBA) or period when 50% of plants were at anthesis (DAA) for 2017 (left panel) and

948 2018 (right panel). Note the different night and day periods on the primary and secondary x-
949 axes.

950 Figure 5. Relationship of rate of O_2 consumption at 25°C ($R_{dark\_}O_2^{25}$) with average daily
951 minimum temperature (open circles and solid lines) or maximum temperature (open sqaures
952 and dashed lines) of the 1–3 day period when 50% of plants were at anthesis (DAA) for 2017
953 (left panel) and 2018 (right panel).

954 Figure 6. Relative change in mean yield of 20 genotypes for time of sowing (TOS) 2 (white
955 bars) and TOS3 (black bars) compared to TOS1 in 2017 (a) and 2018 (b). Spearman's Rank
956 correlations of the relative change in yield of TOS2 and TOS3 from TOS1 were 0.84 (P<0.001)
957 for 2017 and 0.93 for 2018.

Table legends

Table 1. Environmental conditions during defined periods for each time of sowing (TOS) during 2017 and 2018.

Table 2. Analysis of variance of thermal acclimation-related traits for wheat genotypes grown under three thermal regimes, achieved by varying time of sowing (TOS) during 2017 and 2018.

Table 3. Back-transformed means of the ratios of leaf dark respiration rates at 25°C (CO_2 efflux, $R_{dark\_}CO_2^{25}$) to net, area-based, CO_2 assimilation rates measured at 25°C (A^{25}) and maximum carboxylation capacity of photosynthesis at 25°C (V_{cmax}^{25}) of six wheat genotypes grown under three thermal regimes (by varying time of sowing, TOS) during 2017 and 2018. n=4.

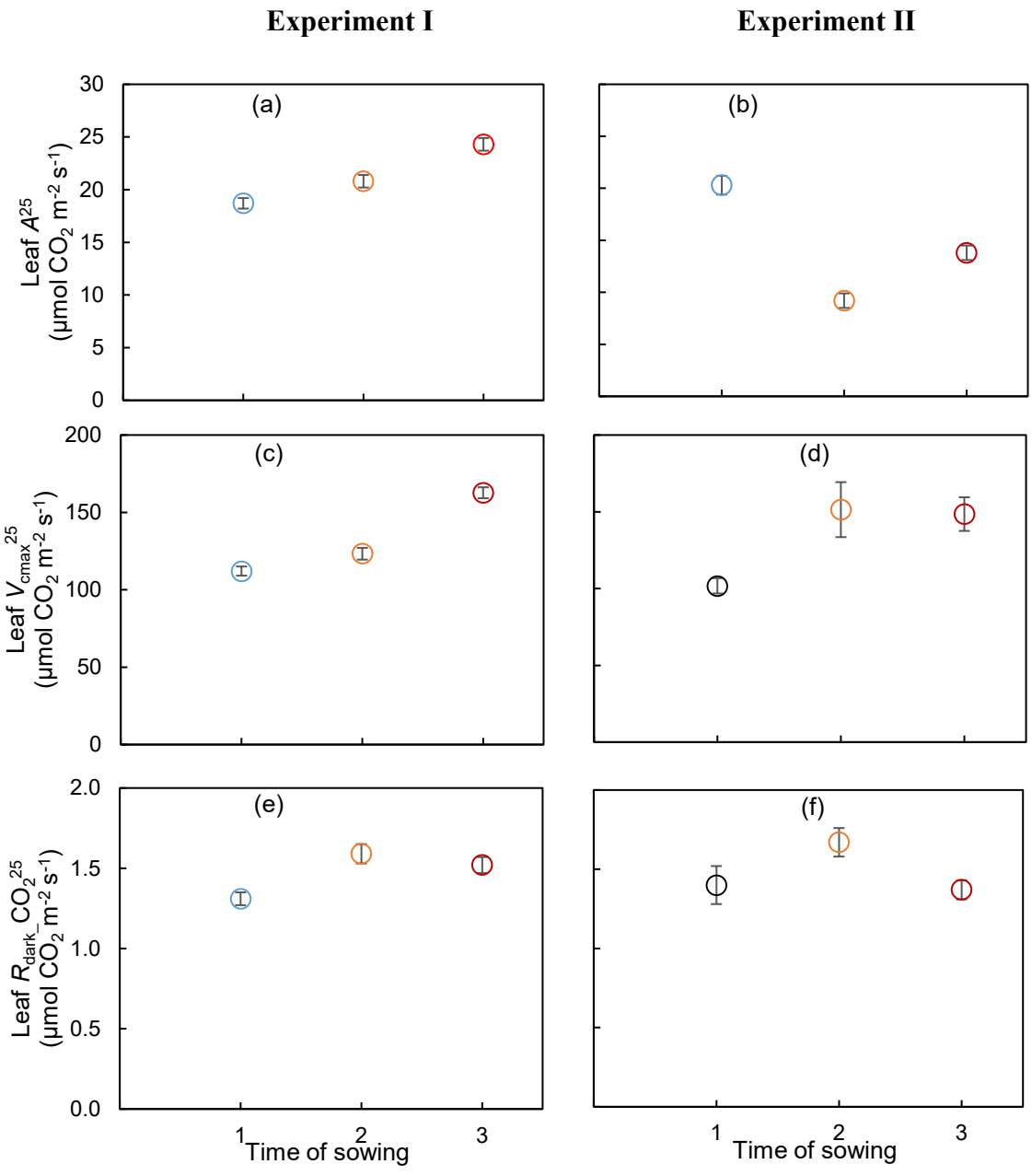

Figure 1. Mean rates of area-based net CO_2 assimilation rates at 25°C (A^{25}), maximum carboxylation capacity of photosynthetic capacity (V_{cmax}^{25}), and leaf dark respiration at 25°C taken as rate of CO_2 efflux ($R_{dark}\_CO_2^{25}$) for six selected wheat genotypes. Genotypes were grown under three thermal regimes (by varying time of sowing, TOS) during 2017 (a, c and e) and 2018 (b, d and f). Values are the mean of four plants (±standard error of mean).

978

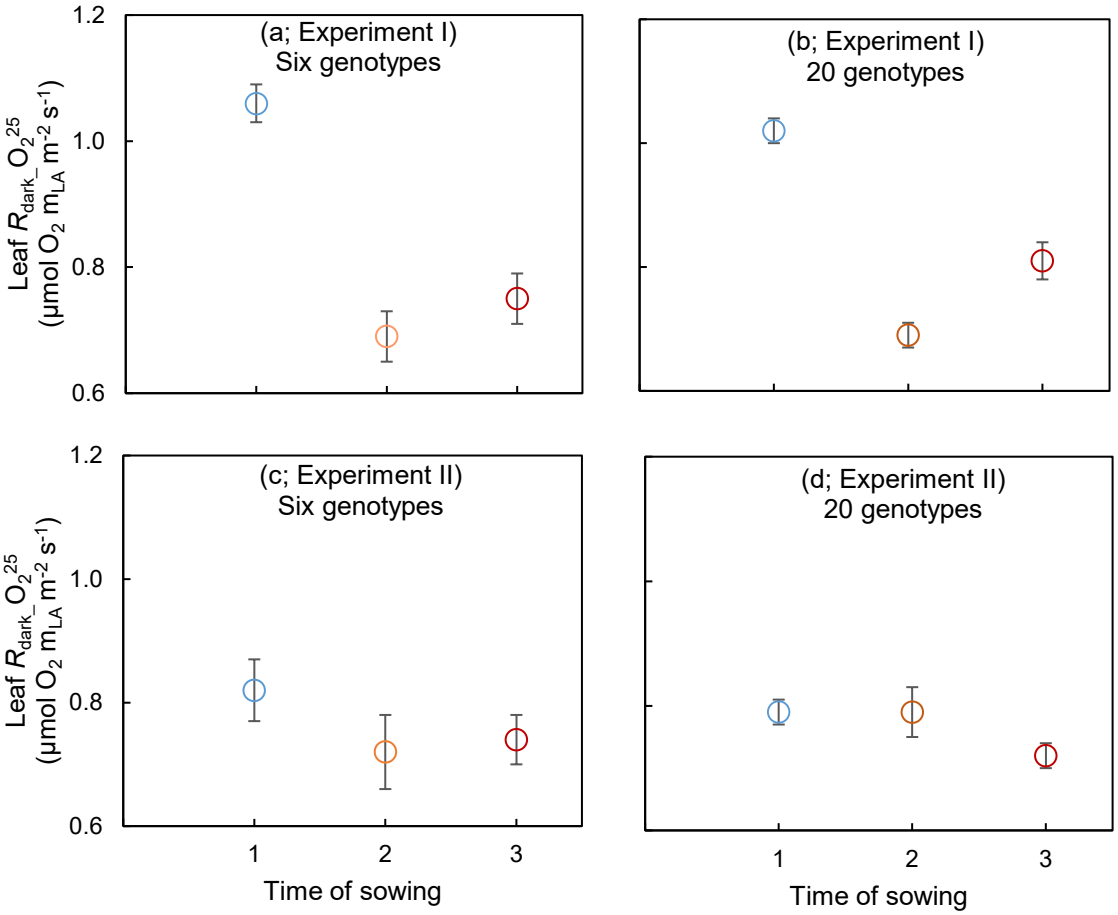

979

980

981 Figure 2. Mean rates of leaf dark respiration on O_2 consumption basis at 25°C ($R_{dark\_}O_2^{25}$) for

982 six selected and the whole set of 20 wheat genotypes. Genotypes were grown under three

983 thermal regimes (by varying time of sowing, TOS) during 2017 (a, b) and 2018 (c, d). Values

984 are the mean of four plants (±standard error of mean).

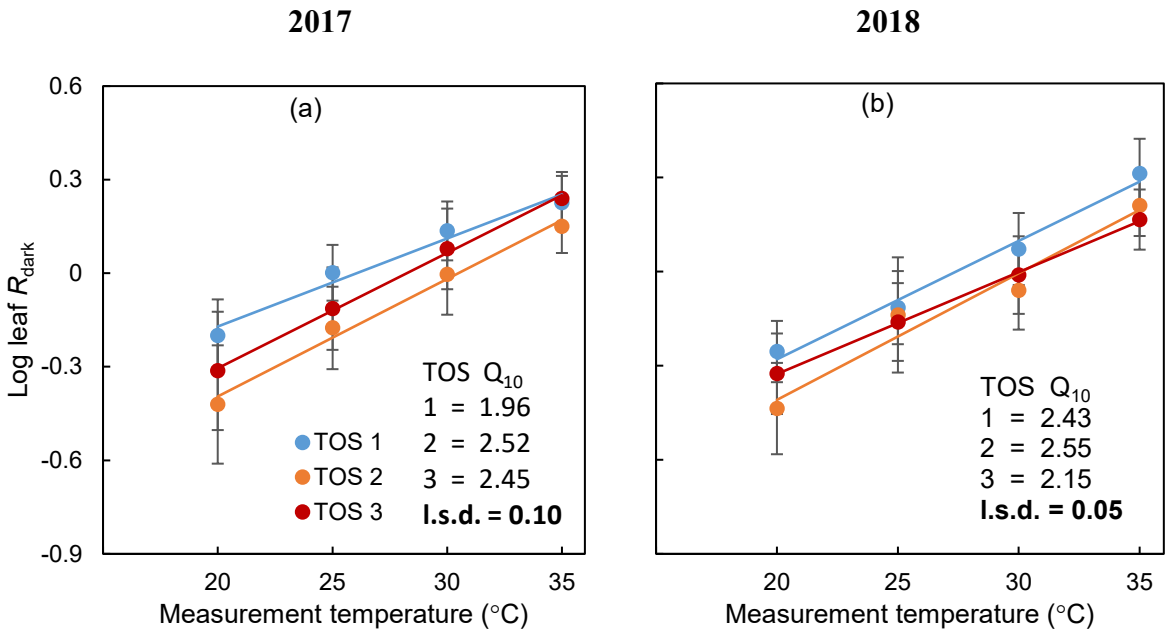

Figure 3. Mean temperature response of leaf dark respiration (O_2 consumption; values shown on a log scale) expressed per leaf area (R_{dark}) of 20 wheat genotypes grown under three thermal regimes (by varying time of sowing, TOS) during 2017 (a) and 2018 (b). Values are the means of four plants (±standard deviation) from each of 20 genotypes at the different TOS. Treatments (or TOS) are significantly different (P<0.05) if the difference in their Q_{10} values is greater than the indicated least significant difference (l.s.d.) value. Parameter estimates of the log-transformed instantaneous leaf R_{dark}-temperature responses are given in Table S6.

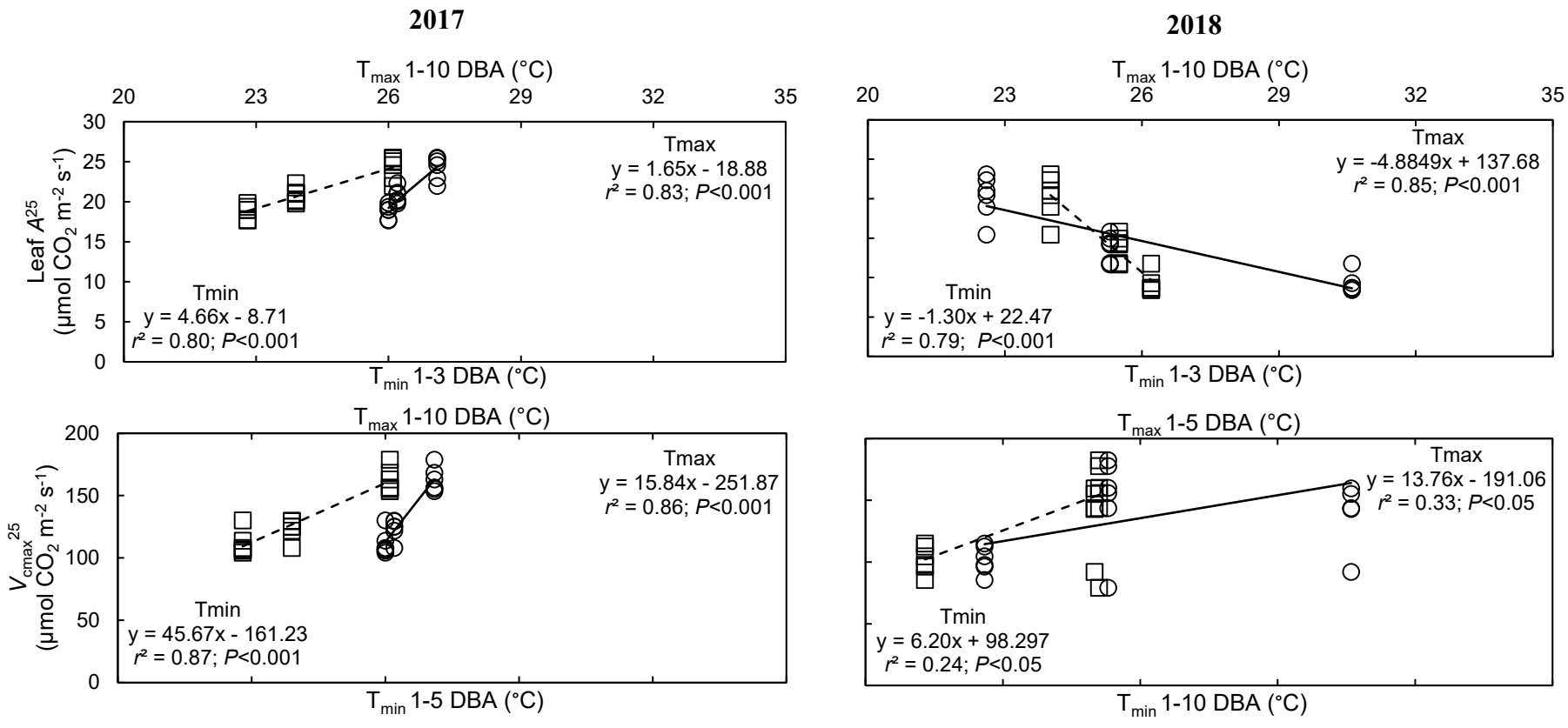
2017
2018
T_{max} 1-10 DBA (°C)
Leaf A^{25} (µmol CO_2 m^{-2} s^{-1})
Tmax
y = 1.65x - 18.88
r^2 = 0.83; P<0.001
Tmin
y = 4.66x - 8.71
r^2 = 0.80; P<0.001
T_{min} 1-3 DBA (°C)
Tmax
y = -4.8849x + 137.68
r^2 = 0.85; P<0.001
Tmin
y = -1.30x + 22.47
r^2 = 0.79; P<0.001
T_{max} 1-10 DBA (°C)
V_{cmax}^{25} (µmol CO_2 m^{-2} s^{-1})
Tmax
y = 15.84x - 251.87
r^2 = 0.86; P<0.001
Tmin
y = 45.67x - 161.23
r^2 = 0.87; P<0.001
T_{min} 1-5 DBA (°C)
T_{max} 1-5 DBA (°C)
Tmax
y = 13.76x - 191.06
r^2 = 0.33; P<0.05
Tmin
y = 6.20x + 98.297
r^2 = 0.24; P<0.05
T_{min} 1-10 DBA (°C)

994

995

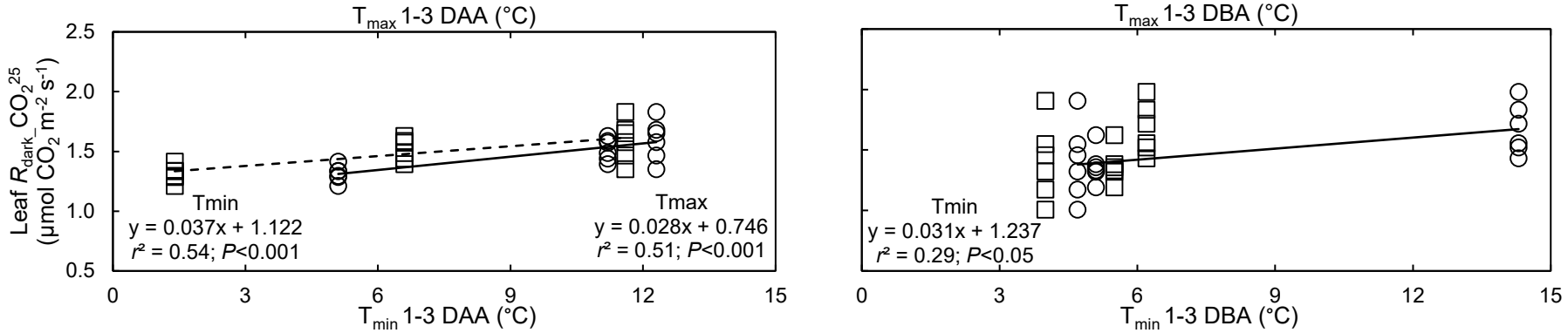

996

997 Figure 4. Relationship of mean area-based leaf net CO_2 assimilation rate (A^{25}), maximum carboxylation capacity of photosynthetic capacity

998 (V_{cmax}^{25}) and rate of CO_2 efflux ($R_{dark}\_CO_2^{25}$) at 25°C with average minimum temperature (open circles and solid lines) or maximum temperature

999 (open sqaures and dashed lines) of period before 50% of plants had achieved anthesis (DBA) or period when 50% of plants were at anthesis (DAA)

1000 for 2017 (left panel) and 2018 (right panel). Note the different night and day periods on the primary and secondary x-axes.

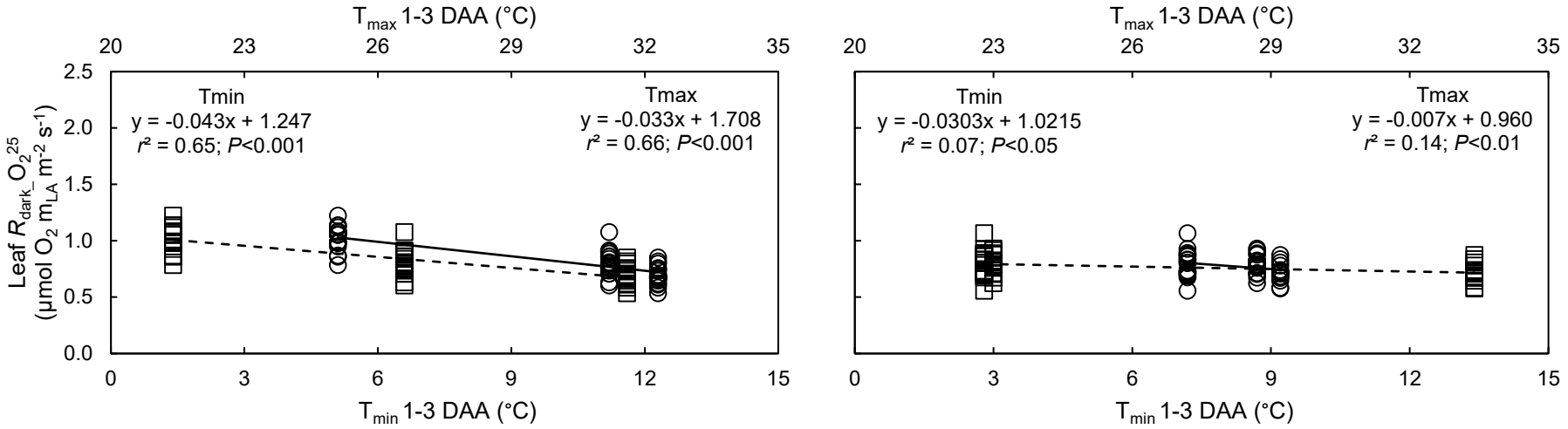

1001

1002 Figure 5. Relationship of rate of O_2 consumption at 25°C ($R_{dark}\_O_2^{25}$) with average daily minimum temperature (open circles and solid lines) or

1003 maximum temperature (open sqaures and dashed lines) of the 1–3 day period when 50% of plants were at anthesis (DAA) for 2017 (left panel)

1004 and 2018 (right panel).

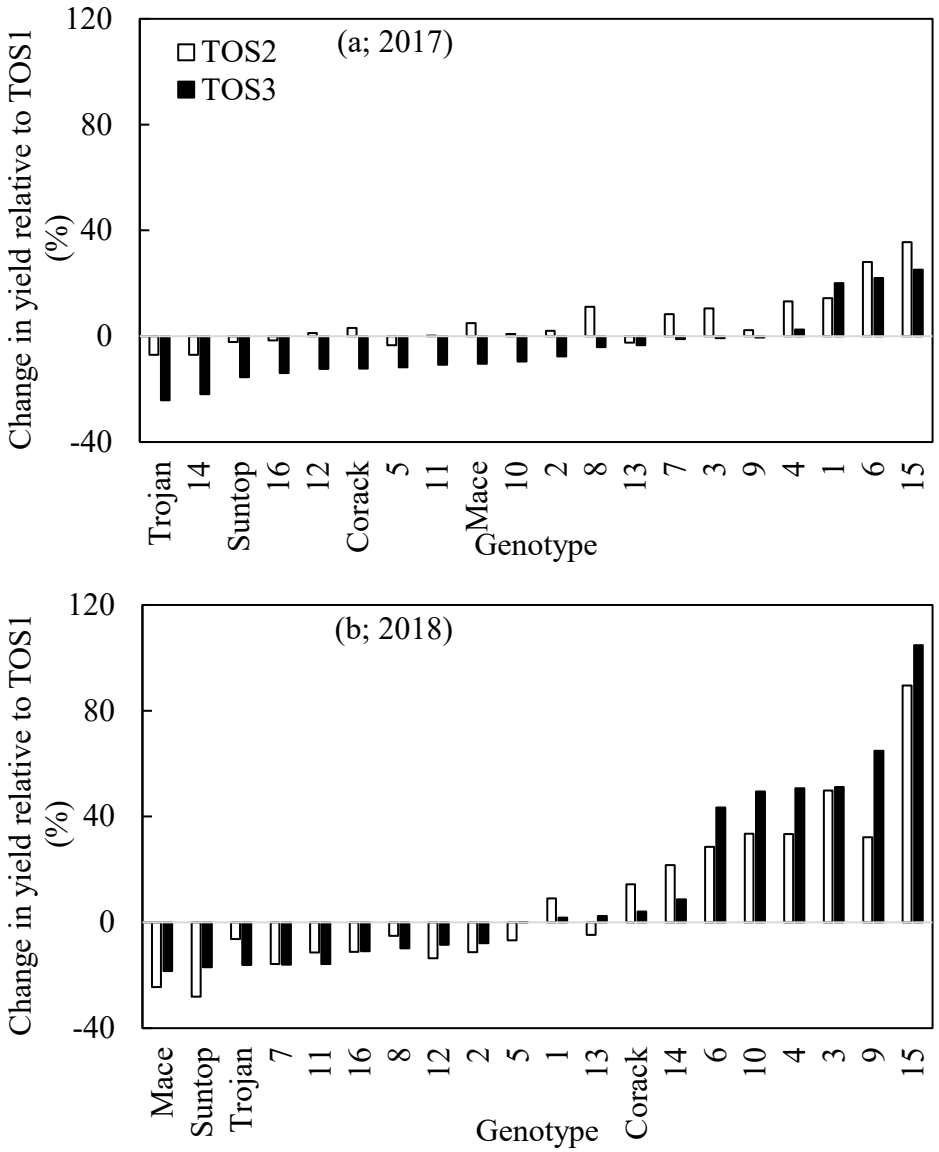

Figure 6. Relative change in mean yield of 20 genotypes for time of sowing (TOS) 2 (white bars) and TOS3 (black bars) compared to TOS1 in 2017 (a) and 2018 (b). Spearman's Rank correlations of the relative change in yield of TOS2 and TOS3 from TOS1 were 0.84 (P<0.001) for 2017 and 0.93 (P<0.001) for 2018.

1011 Table 1. Environmental conditions during defined periods for each time of sowing (TOS) during 2017 and 2018.

Weather parameter/Period	TOS	Average T_{max}/T_{min}[1] (°C)		Total rainfall (mm)		Total solar radiation (kWh m^{-2})		PAR[2] (µmol (photons) m^{-2} s^{-1})	
		2017	2018	2017	2018	2017	2018	2017	2018
Sowing to anthesis[3]	1	16.8/4.7	16.4/3.5	123	69	477	420	---	---
	2	17.7/4.8	17.4/3.9	90	73	499	491	---	---
	3	18.7/5.6	20.1/5.2	97	67	502	606	---	---
Anthesis[4]	1	21.4/ 5.1	22.8/7.2	0	0	14	15	1394	2331
	2	31.6/12.3	23.0/8.7	0	0	19	20	1934	1706
	3	26.6/11.2	33.4/9.2	0	0	18	19	1632	2041

1012 [1]Average daily maximum or minimum temperature, actual daily temperature and other environmental variables are given in supplementary Table
1013 S2. [2]Mean maximum photosynthetically active radiation measured with Licor 6400XTs light sensors during gas exchange measurements. [3]Data
1014 from closest Australian Bureau of Meteorology weather station in 2017 and on-site weather station in 2018; [4]Mean values of the three-day period
1015 when physiological measurements were taken and during which at least 50% of plants had visible anther.

Table 2. Analysis of variance of thermal acclimation-related traits for wheat genotypes grown under three thermal regimes, achieved by varying time of sowing (TOS) during 2017 and 2018.

	Genotype		TOS		Genotype x TOS	
	d.f.	v.r	d.f.	v.r	d.f.	v.r
2017						
Six genotypes						
A^{25}	5	1.03^{ns}	2	**25.48*****	10	0.46^{ns}
$V_{cmax}{}^{25}$	5	**3.05***	2	**66.72*****	10	0.45^{ns}
$R_{dark\_}CO_2{}^{25}$	5	0.45^{ns}	2	**7.28****	10	0.98^{ns}
$R_{dark\_}O_2{}^{25}$	5	1.73^{ns}	2	**31.55*****	10	0.34^{ns}
20 genotypes						
$R_{dark\_}O_2{}^{20}$	19	0.52^{ns}	2	**14.28*****	38	0.27^{ns}
$R_{dark\_}O_2{}^{25}$	19	1.53^{ns}	2	**50.43*****	38	0.49^{ns}
$R_{dark\_}O_2{}^{30}$	19	1.34^{ns}	2	**28.18*****	38	0.54^{ns}
$R_{dark\_}O_2{}^{35}$	19	**1.95***	2	**19.58*****	38	0.60^{ns}
2018						
Six genotypes						
A^{25}	5	1.54^{ns}	2	**49.56*****	10	0.93^{ns}
$V_{cmax}{}^{25}$	5	**4.15****	2	**10.89*****	10	**2.18***
$R_{dark\_}CO_2{}^{25}$	5	2.07^{ns}	2	**10.21*****	10	0.45^{ns}
$R_{dark\_}O_2{}^{25}$	5	0.05^{ns}	2	0.96^{ns}	10	0.42^{ns}
20 genotypes						
$R_{dark\_}O_2{}^{20}$	19	**1.72***	2	**46.45*****	38	1.09^{ns}
$R_{dark\_}O_2{}^{25}$	19	0.47^{ns}	2	2.52^{ns}	38	0.57^{ns}
$R_{dark\_}O_2{}^{30}$	19	1.02^{ns}	2	**26.19*****	38	0.84^{ns}
$R_{dark\_}O_2{}^{35}$	19	1.38^{ns}	2	**44.94*****	38	0.79^{ns}

A^{25} (μmol CO_2 m^{-2} s^{-1}), net CO_2 assimilation rate measured at 25°C; $V_{cmax}{}^{25}$ (μmol CO_2 m^{-2} s^{-1}) maximum carboxylation capacity of photosynthetic capacity at 25°C; $R_{dark\_}CO_2{}^{25}$ (μmol CO_2 m^{-2} s^{-1}), dark respiration (CO_2 efflux) rate measured at 25°C; $R_{dark\_}O_2$ (μmol O_2 $m_{LA}{}^{-2}$ s^{-1}), dark respiration (O_2 consumption) rate measured at 20, 25, 30 or 35°C. The respiration flux values are area-based. ^{ns}=not significant. *$P < 0.05$. **$P < 0.01$. ***$P < 0.001$. Significant effects are indicated in bold.

Table 3. Back-transformed means of the ratios of leaf dark respiration rates at 25°C (CO_2 efflux, $R_{dark}\_CO_2^{25}$) to net, area-based, CO_2 assimilation rates measured at 25°C (A^{25}) and maximum carboxylation capacity of photosynthesis at 25°C (V_{cmax}^{25}) of six wheat genotypes grown under three thermal regimes (by varying time of sowing, TOS) during 2017 and 2018. n=4.

Time of sowing	2017		2018	
	$R_{dark}\_CO_2^{25}$:A^{25}	$R_{dark}\_CO_2^{25}$:V_{cmax}^{25}	$R_{dark}\_CO_2^{25}$:A^{25}	$R_{dark}\_CO_2^{25}$:V_{cmax}^{25}
1	0.072	0.012	0.075	0.015
2	0.078	0.013	0.215	0.013
3	0.063	0.009	0.104	0.010
Mean	0.071	0.012	0.132	0.013
l.s.d (F pr.)				
TOS	**0.010***	**0.001*****	**0.044*****	**0.005***
Other terms				
Genotype	0.014^{ns}	0.002^{ns}	0.063^{ns}	0.007^{ns}
Genotype x TOS	0.024^{ns}	0.003^{ns}	0.108^{ns}	0.012^{ns}

Levels of significant differences for the treatment terms are indicated by ^{ns}=not significant, P>0.05; *P < 0.05; ***P < 0.001.

Supplementary Information.

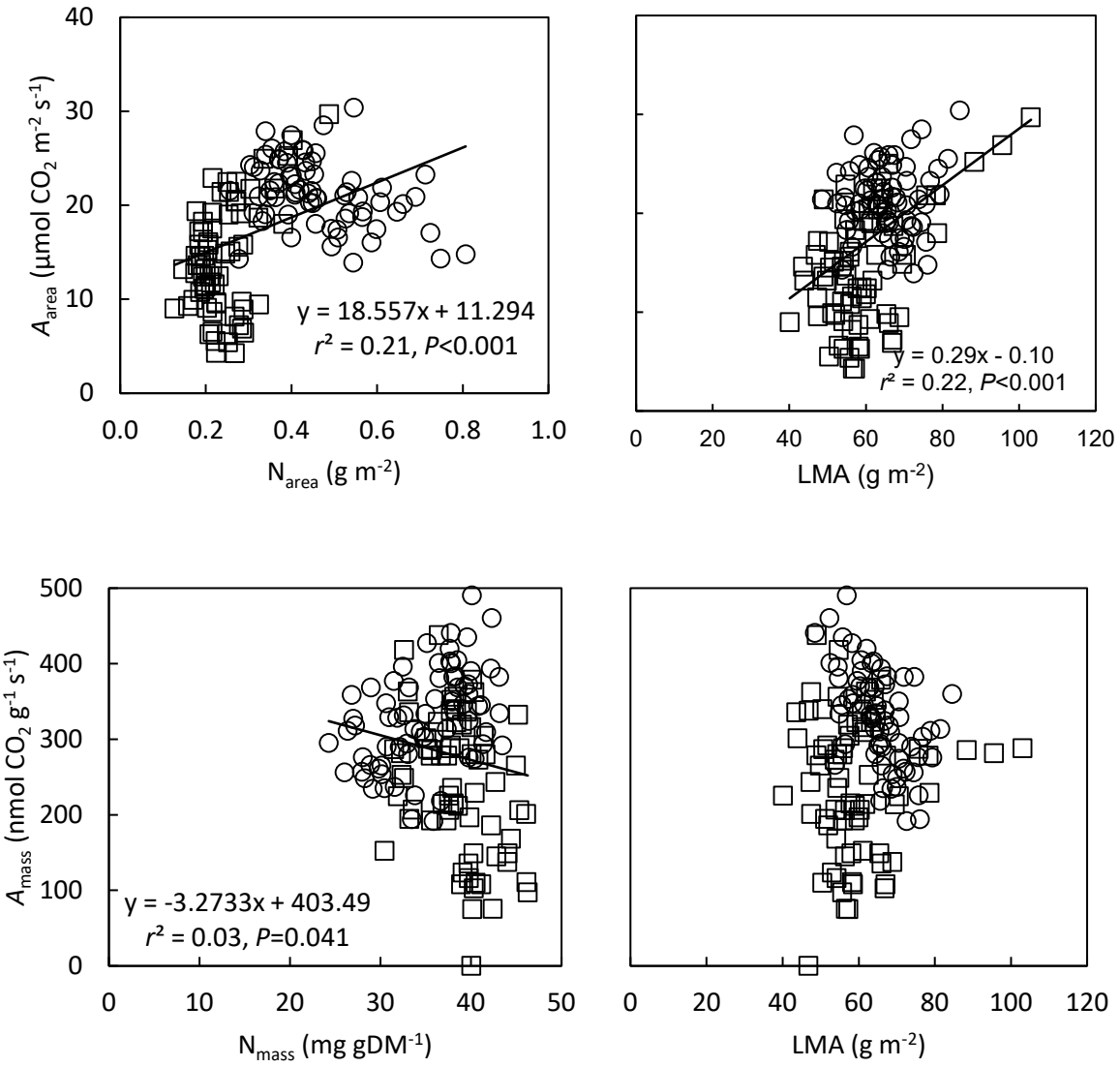

Supplementary Figure S1. Bivariate plots of net CO_2 assimilation rates measured at 25°C (area based, A_{area}^{25}, top panels; and mass based, A_{mass}^{25}, bottom panels) with leaf N (area based, N_{area}, top left panel; and mass based, N_{mass}, bottom left panel) and leaf mass per unit area (LMA, right panels). Circles and squares represent data from 2017 and 2018, respectively.

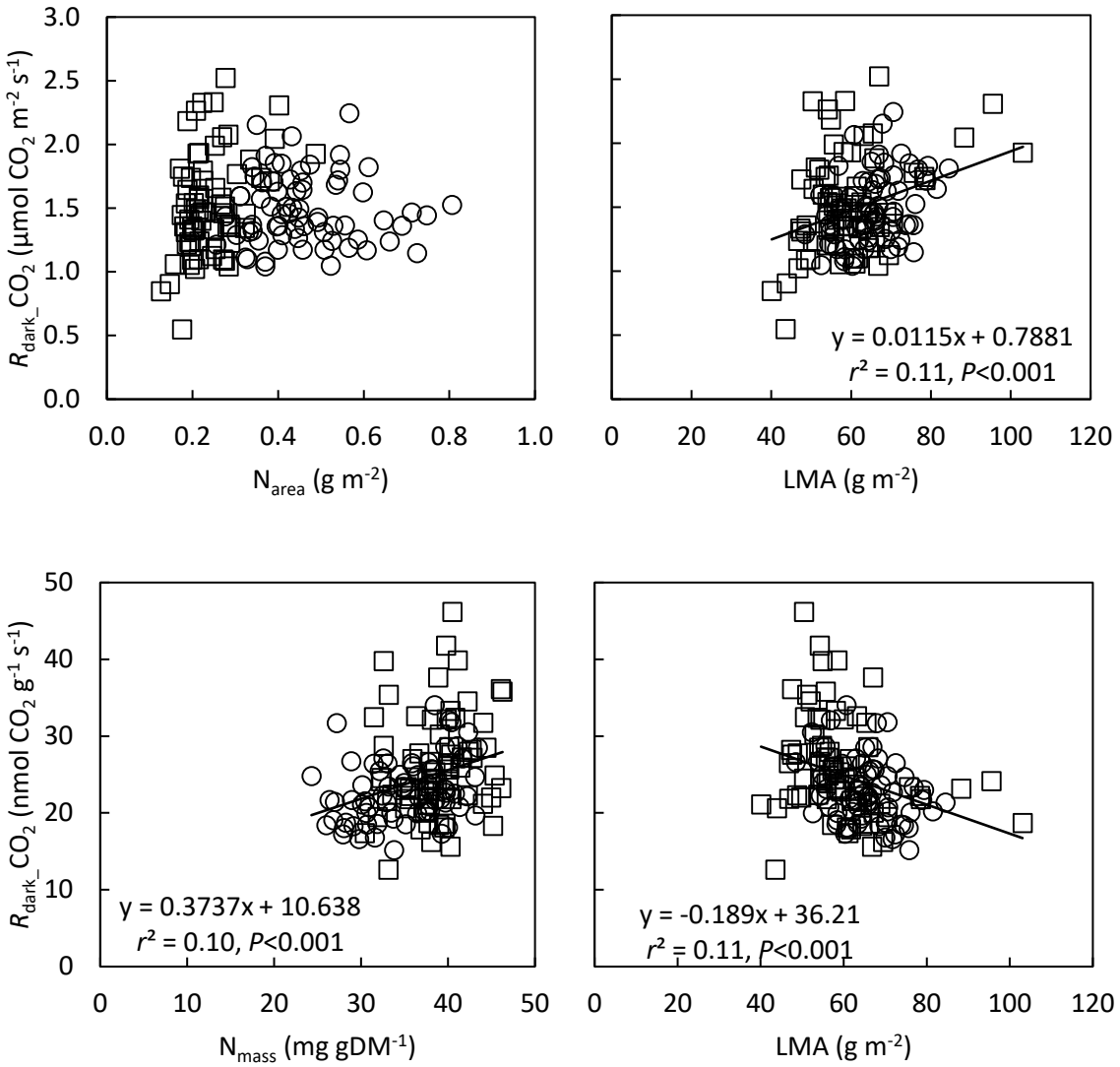

Supplementary Figure S2. Bivariate plots of leaf dark respiration taken as rate of CO_2 efflux ($R_{dark\_}CO_2$) measured at 25°C (area based, top panels; and mass based, bottom panels) with leaf N (area based, N_{area}, top left panel; and mass based, N_{mass}, bottom left panel) and leaf mass per unit area (LMA, right panels). Circles and squares represent data from 2017 and 2018, respectively.

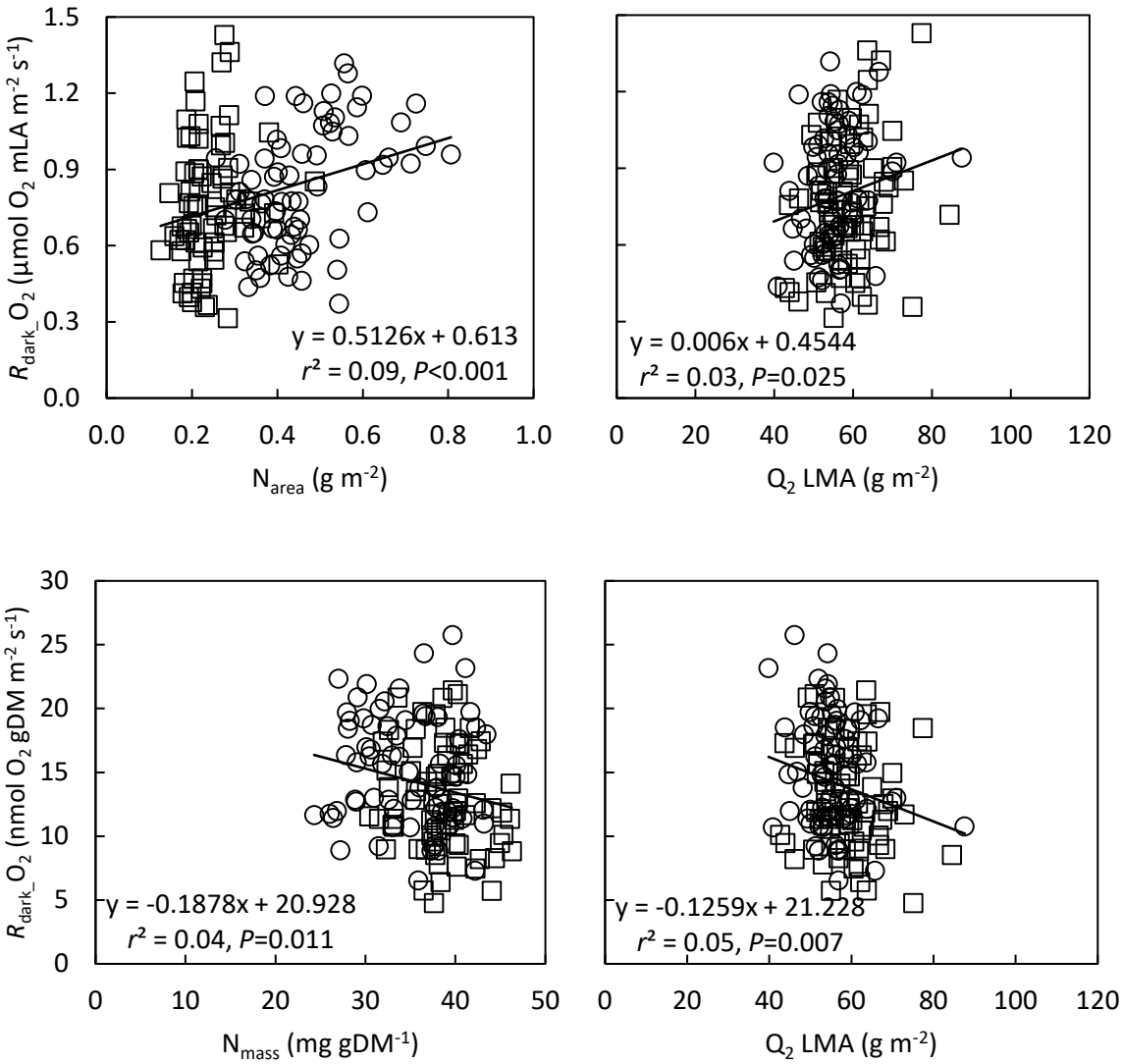

Supplementary Figure S3. Bivariate plots of leaf dark respiration taken as rate of O_2 consumtion ($R_{dark\_}O_2$) measured at 25°C (area based, top panels; and mass based, bottom panels) with leaf N (area based, N_{area}, top left panel; and mass based, N_{mass}, bottom left panel) and leaf mass per unit area (LMA, right panels). Circles and squares represent data from 2017 and 2018, respectively.

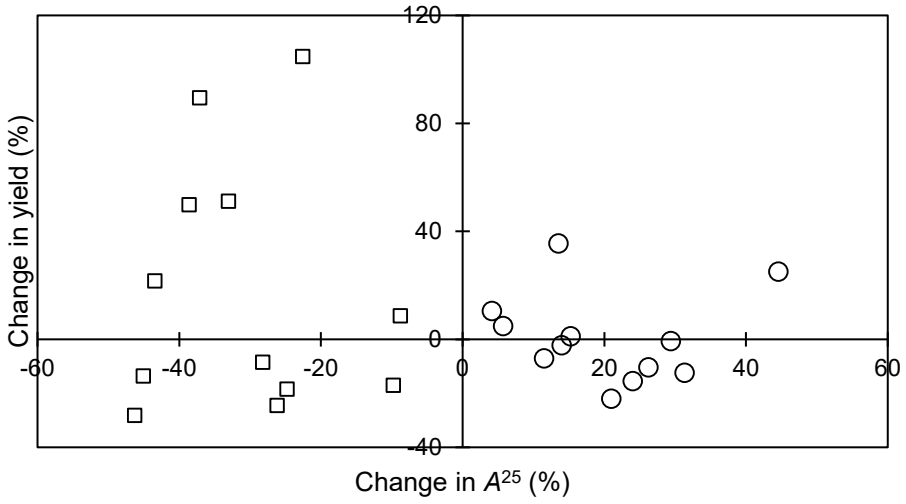

22

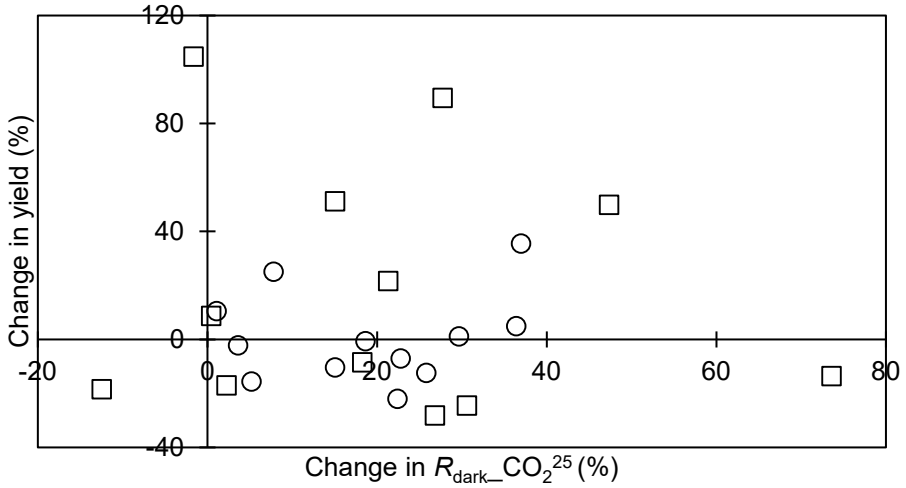

23

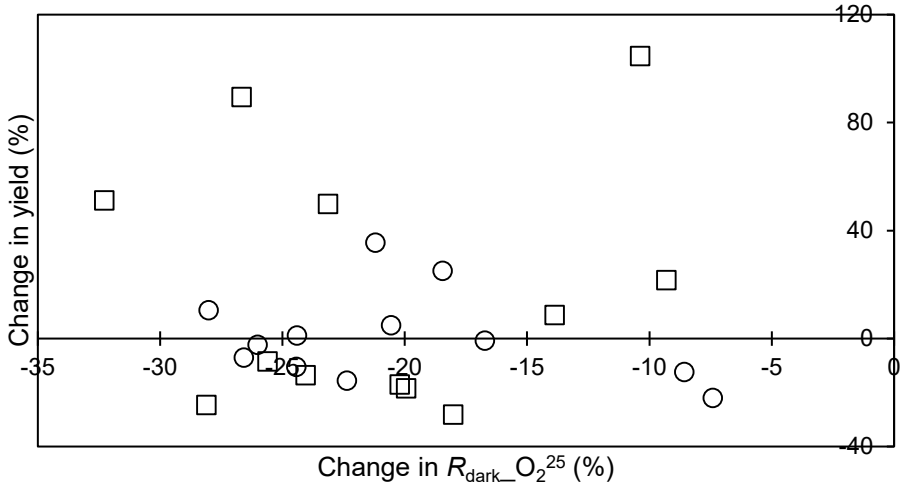

24

25 Supplementary Figure S4. Plots of change in mean grain yield versus changes in mean net
26 CO_2 assimilation rate (A^{25}, top panel) and leaf dark respiration (rate of CO_2 efflux,
27 $R_{dark}\_CO_2^{25}$, middle panel; and rate of O_2 consumption $R_{dark}\_O_2^{25}$, bottom panel). Circles and
28 squares represent data from 2017 and 2018, respectively.

Supplementary Table S1. Genotypes used in study.

Entry	Name (Origin)	Pedigree	Note
1	PBI09C004-BC-DH43 (USyd)	Berkut/2/Berkut/35883 M500110	Backcross of a hexaploid wheat to a heat tolerant tetraploid *T. dicoccum* and a hexaploid type selected
2	PBI09C009-BC-DH51 (USyd)	Sokoll/2/Sokoll/ 35888 M 500132	Same as above
3	PBI09C026-BC-DH41 (USyd)	Waxwing*2/Kiritati /3/Waxwing*2/Kiritati /2/ 35888 M 500132	Same as above
4	ACIAR09PBI C04-17C-DH10 (USyd)	PBW550//C80.1/*2Batavia	Cross of heat tolerant Indian cultivar with rust resistant sources
5	ACIAR09PBI C38-115C-DH9 (USyd)	PBW343+L24+LR28/Lang	Same as above
6	ACIAR09PBI C29-51C-DH1 (USyd)	DBW16/Sunstate	Same as above
7	ACIAR09PBI C27-0C-0N-3N (USyd)	DBW16/Annuello	Same as above
8	ACIAR09PBI C26-0C-0N-2N (USyd)	DBW16/Gladius	Same as above
9	PBI07C101-DH64 (USyd)	ISR 812.8/Carinya	Heat tolerant Mexican hexaploid landrace cross to Australian cultivar
10	PBI07C101-DH154 (USyd)	ISR 812.8/Carinya	Same as above
11	PBI07C201-BC-DH66 (USyd)	Ventura/Ido 637//Ventura	Low phytate mutant crossed to Australian cultivar - pre-screened for heat tolerance
12	8:ZWW11 (CIMMYT)	D67.2/P66.270//AE.Squarrosa (320)/3/Cunningham/4/Vorb	Heat tolerant in Mexico (Ciudad Obregon) and Narrabri, Australia
13	77:ZWW11 (CIMMYT)	SLVS/Attila//WBLL1*2/3/Gondo/CBRD	Heat tolerant in Mexico (Ciudad Obregon) and Narrabri, Australia
14	45:ZIZ12 (ICARDA)	Hubara-8///Mon's'/Ald's'//Bow's'	Heat tolerant hexaploid; good performance in Sudan and Narrabri
15	267:ZWB13 (CIMMYT)	RAC 1192/4/2*Attila/3/Weaver*2/TSC//Weaver	Heat tolerant hexaploid; good performance in Mexico (Ciudad Obregon) and Narrabri, Australia
16	PBI09C009-BC-DH56 (USyd)	Sokoll/2/Sokoll/35888 M 500132	Backcross of a hexaploid wheat to a heat tolerant tetraploid T. dicoccum and a hexaploid type selected
17	Corak (AGT)		Commercial cultivar, released in 2012
18	Suntop (AGT)		Commercial cultivar, released in 2012
19	Trojan (LongReach)		Commercial cultivar, released in 2013
20	Mace (AGT)	Wyalkatchem/Stylet//Wyalkatchem	Commercial cultivar, released in 2008

USyd, The University of Sydney, Australia; CIMMYT, The International Maize and Wheat Improvement Center, Mexico; ICARDA, The International Centre for Agricultural Research in the Dry Areas, Syria; AGT, Australian Grains Technology, Australia; LongReach, LongReach Plant Breeders, Australia.

Supplementary Table S2. Daily environmental conditions at anthesis for each time of sowing (TOS) during 2017 and 2018.

Weather parameter/Period	Day	T_{max}/T_{min} (°C)		Total solar radiation (kWh m^{-2})		Maximum photosynthetically active radiation[1] (µmol (photons) m^{-2} s^{-1})	
		2017	2018	2017	2018	2017	2018
TOS1	1	18.4/ 1.2	24.1/10.6	5.83	3.40	2119	2331
	2	28.1/ 8.4	21.1/ 7.4	5.19	6.10	668	---
	3	17.6/ 5.7	23.3/ 3.7	3.49	5.34	---	---
TOS2	1	31.0/11.3	19.7/ 8.7	6.87	3.51	1924	1442
	2	32.9/10.9	19.1/10.3	6.69	2.72	1943	1970
	3	30.9/14.8	30.3/ 7.1	4.96	5.62	---	---
TOS3	1	29.0/10.9	30.2/ 4.7	4.85	7.07	1552	2041
	2	26.4/13.1	32.8/ 9.6	4.23	6.80	1712	---
	3	24.5/ 9.6	37.3/13.4	5.06	4.45	---	---

[1]Photosynthetically active radiation measured with Licor 6400XTs light sensors during gas exchange measurements.

Supplementary Table S3. Rainfall and irrigation data from sowing to anthesis for different times of sowing (TOS) during 2017 and 2018.

Water supply (mm)	TOS1	TOS2	TOS3
2017[1]			
Rainfall	123	90	97
Irrigation amount	62	62	62
Total water supplied	**185**	**152**	**159**
2018			
Rainfall	69	73	67
Irrigation amount	148	148[2]	168[2]
Total water supplied	**217**	**221**	**235**

[1]data from closest Australian Bureau of Meteorology weather station for 2017 and on-site weather station for 2018. [2]There was a brief period of water deficit stress (with visible signs of leaf rolling) prior to and including the period of physiological measurements of TOS2 and TOS3 in 2018 that is not reflected by these irrigation data.

Supplementary Table S4. **2017**. Proportional change in leaf dark respiration (rate of oxygen consumption expressed per unit of leaf area) for a 10°C increase in temperature (Q_{10}) between 20 and 35°C of 20 wheat genotypes grown under three thermal regimes, achieved by varying time of sowing (TOS), at anthesis.

Genotype	Q_{10}			
	TOS1	TOS2	TOS3	Mean
1	2.08	**2.91**	**2.48**	**2.49**
2	1.88	**2.58**	**2.25**	**2.24**
3	2.13	**2.68**	**2.76**	**2.52**
4	2.02	**2.28**	2.10	**2.13**
5	2.11	**2.47**	**2.36**	**2.31**
6	1.78	**2.43**	**2.43**	**2.21**
7	2.05	**2.26**	**2.47**	**2.26**
8	1.92	**2.79**	**3.19**	**2.63**
9	1.82	**2.72**	**2.68**	**2.41**
10	1.89	**2.69**	**2.09**	**2.23**
11	1.93	**2.52**	**2.31**	**2.25**
12	1.92	**2.54**	**2.49**	**2.32**
13	1.71	**2.18**	**2.19**	**2.03**
14	1.79	**2.39**	**2.59**	**2.26**
15	1.83	**2.39**	**2.24**	**2.15**
16	2.09	**2.70**	**2.33**	**2.37**
Corak	2.18	**2.47**	**2.40**	**2.35**
Suntop	2.08	**2.70**	**2.59**	**2.46**
Trojan	1.83	**2.52**	**2.37**	**2.24**
Mace	2.12	2.11	**2.71**	**2.31**
Mean	**1.96**	**2.52**	**2.45**	
l.s.d. Genotype		$0.27^{P=0.003}$		
l.s.d. TOS		$0.10^{P\leq0.001}$		
l.s.d. Genotype x TOS		$0.47^{P=0.191}$		

Significant change in Q_{10} from TOS1 to TOS2 or TOS3 is highlighted in bold.

Supplementary Table S5. **2018**. Proportional change in leaf dark respiration (rate of oxygen consumption expressed per unit of leaf area) for a 10°C increase in temperature (Q_{10}) between 20 and 35°C of 20 wheat genotypes grown under three thermal regimes, achieved by varying time of sowing (TOS), at anthesis.

Genotype	Q_{10}			
	TOS1	TOS2	TOS3	Mean
1	2.44	2.40	1.**88**	**2.24**
2	2.77	**2.08**	**2.34**	**2.40**
3	2.15	**3.22**	**2.21**	**2.53**
4	2.38	2.37	**2.04**	**2.26**
5	2.70	**2.44**	**2.21**	**2.45**
6	2.38	**2.60**	**2.20**	**2.39**
7	2.22	**2.52**	2.22	**2.32**
8	2.27	**2.47**	**1.85**	**2.20**
9	2.89	**2.19**	**2.56**	**2.55**
10	2.18	**2.49**	**2.12**	**2.26**
11	2.43	**3.07**	**1.88**	**2.46**
12	2.71	2.73	**2.25**	**2.56**
13	2.48	2.52	**2.00**	**2.33**
14	2.02	**2.59**	2.04	**2.22**
15	2.19	**2.46**	**1.99**	**2.21**
16	2.57	2.52	**2.09**	**2.39**
Corak	2.36	**2.70**	**2.23**	**2.43**
Suntop	2.40	2.59	**2.03**	**2.34**
Trojan	2.75	**2.29**	**2.53**	**2.52**
Mace	2.25	**2.77**	2.23	**2.42**
Mean	**2.43**	**2.55**	**2.15**	
l.s.d. Genotype		$0.14^{P\leq0.001}$		
l.s.d. TOS		$0.05^{P\leq0.001}$		
l.s.d. Genotype x TOS		$0.24^{P\leq0.001}$		

Significant change in Q_{10} from TOS1 to TOS2 or TOS3 is highlighted in bold

Supplementary Table S6. Parameter estimates of log-transformed instantaneous leaf dark respiration-temperature responses of 20 wheat genotypes grown under three thermal regimes, achieved by varying time of sowing (TOS) during 2017 and 2018. Values of leaf dark respiration presented are based on rate of O_2 consumption expressed per unit of leaf area of 20 genotypes.

Experiment	R_{dark} O_2	slope	intercept	Q_{10}
2017				
TOS1	0.041	0.028***	-0.74***	1.96
TOS2	**-0.111**	**0.038*** **	**-1.15*** **	**2.52**
TOS3	**-0.027**	**0.037*** **	**-1.04*** **	**2.45**
2018				
TOS1	0.003	0.038***	-1.04***	2.43
TOS2	-0.106	**0.040*** **	**-1.22*** **	2.55
TOS3	-0.083	**0.033*** **	**-0.98*** **	**2.15**

Log $R_{dark\_}O_2$ (μmol O_2 m_{LA}^{-2} s^{-1}), log-transformed dark respiration (O_2 consumption) rate measured at 25°C. Slopes and intercept values are the means of 20 wheat genotypes with four replicates across four temperatures (20, 25, 30 and 35°C). ***$P < 0.001$. Parameter estimates siginificantly different from TOS1 are indicated in bold.

Table S7. Estimates of parameters and goodness of fit for equations of multiple linear regressions of leaf traits explained by environmental variables over the 1–3 days of 50% anthesis of 6–20 wheat genotypes grown in 2017 and 2018, each with three different thermal regimes (achieved by varying time of sowing).

			Six genotypes			
Leaf traits	Constant	Average T_{max} (°C)[1]	Average T_{min} (°C)[2]	Total solar radiation (kWh m^{-2})	Mean photosynthetically active radiation (µmol (photons) m^{-2} s^{-1})	Goodness of fit (r^2)
A^{25}	48.1***	-0.212	3.117***	-2.909***	-0.002	0.72***
$R_{dark}\_CO_2^{25}$	1.092**	-0.021*	0.030	0.032	0.000	0.25*
$R_{dark}\_O_2^{20}$	1.197***	0.005	0.002	-0.054***	0.000	0.64***
$R_{dark}\_O_2^{25}$	1.471***	0.000	-0.027*	-0.028	0.000	0.55***
$R_{dark}\_O_2^{30}$	2.057***	0.000	-0.005	-0.042	-0.000	0.39***
$R_{dark}\_O_2^{35}$	3.426***	-0.035***	0.046*	-0.080**	0.000	0.55***
			20 Genotypes			
	Constant	Average T_{max} (°C)	Average T_{min} (°C)	Total solar radiation (kWh m^{-2})	Mean photosynthetically active radiation (µmol (photons) m^{-2} s^{-1})	Goodness of fit (r^2)
$R_{dark}\_O_2^{20}$	1.105***	0.003	0.004	-0.039***	-0.000	0.48***
$R_{dark}\_O_2^{25}$	1.331***	-0.009**	-0.016*	-0.003	-0.000	0.41***
$R_{dark}\_O_2^{30}$	2.380***	-0.006	0.030*	-0.074***	-0.000	0.40***
$R_{dark}\_O_2^{35}$	3.451***	-0.030***	0.060***	-0.083***	-0.000	0.41***

[1]Daily Average daily maximum temperature. [2]Average daily minimum temperature. Aesteriks besides parameter estimates and r^2 indicates level of significance (*=P<0.05, **=P<0.01 and ***=P<0.001) based on t. probablity for terms in the regression models and overall F probablity for the full regression model, respectively.

Supplementary Table S8 Leaf mass per unit area (LMA) and leaf nitrogen (N) concentration of six wheat genotypes grown under three thermal regimes, achieved by varying time of sowing (TOS) during 2017 and 2018.

	Genotype (G)	LMA (g m^{-2})			Leaf N_{area} (g m^{-2})			Leaf N_{mass} (mg gDM^{-1})		
		TOS1	TOS2	TOS3	TOS1	TOS2	TOS3	TOS1	TOS2	TOS3
2017										
	3	64	55	62	0.55	0.34	0.38	30	31	40
	12	70	64	67	0.62	0.39	0.41	29	30	40
	14	72	70	66	0.60	0.38	0.40	29	28	40
	15	74	63	65	0.64	0.45	0.38	32	37	38
	Suntop	64	63	58	0.59	0.46	0.38	34	38	41
	Mace	62	72	67	0.53	0.49	0.38	33	36	38
	Mean	**67**	**64**	**64**	**0.59**	**0.42**	**0.39**	**31**	**34**	**40**
l.s.d.										
	Genotype		6^{*}			0.05^{ns}			2^{***}	
	TOS		4^{ns}			0.03^{***}			2^{***}	
	Genotype x TOS		10^{ns}			0.08^{ns}			4^{*}	
2018										
	3	52	55	52	0.24	0.25	0.20	36	44	41
	12	54	60	57	0.25	0.26	0.20	37	42	39
	14	64	62	62	0.34	0.26	0.19	38	41	35
	15	73	53	57	0.34	0.20	0.19	36	37	37
	Suntop	62	53	58	0.28	0.20	0.22	36	36	43
	Mace	64	54	55	0.28	0.23	0.19	36	41	39
	Mean	**61**	**56**	**57**	**0.29**	**0.24**	**0.20**	**37**	**40**	**39**
l.s.d.										
	Genotype		6*			0.04^{ns}			3^{ns}	
	TOS		4*			0.02^{***}			2^{***}	
	Genotype x TOS		11^{ns}			0.06*			5*	

l.s.d.=least significant differences of means (5% level). The superscripts and asterisks indicate the level of significance. ^{ns}=not significant. *P < 0.05. **P < 0.01. ***P < 0.001. n=4.

Supplementary Table S9. **2017:** Parameter estimates of regression models of leaf functional traits (net CO_2 assimilation rate, A^{25}; rate of CO_2 efflux, $R_{dark}\_CO_2^{25}$; and rate of O_2 consumption, $R_{dark}\_O_2^{25}$) with leaf mass per unit area (LMA) or leaf N concentration grouped by time of sowing (TOS). Estimates are given for trait-trait relationships on an area or mass basis.

Structural or chemical traits		Area-based functional leaf traits					
		A^{25}		$R_{dark}\_CO_2^{25}$		$R_{dark}\_O_2^{25}$	
		Intercept	Slope	Intercept	Slope	Intercept	Slope
LMA							
	TOS1	26.6	-0.12	0.93	0.006	1.05	0.000
	TOS2	16.9	0.06	0.18	0.022	**-0.16**	0.015
	TOS3	12.6	**0.18**	0.59	0.014	0.81	-0.001
N							
	TOS1	21.8	-5.16	1.12	0.358	1.21	-0.254
	TOS2	20.2	1.42	0.81	1.879	**0.54**	0.360
	TOS3	17.1	**18.42**	0.90	1.597	1.27	-1.328
V_{cmax}^{25}							
	TOS1	---	---	1.66	-0.003	1.25	-0.002
	TOS2	---	---	0.79	0.007	**0.29**	0.003
	TOS3	---	---	1.33	0.001	1.00	-0.002
		Mass-based functional leaf traits					
		A^{25}		$R_{dark}\_CO_2^{25}$		$R_{dark}\_O_2^{25}$	
		Intercept	Slope	Intercept	Slope	Intercept	Slope
LMA							
	TOS1	724.2	-6.57	34.05	-0.210	35.16	-0.290
	TOS2	587.7	-4.06	26.70	-0.030	**9.82**	**0.044**
	TOS3	574.4	-3.05	32.76	-0.143	28.43	-0.263
N							
	TOS1	139.0	4.53	11.54	0.267	13.93	0.150
	TOS2	283.8	1.26	18.72	0.180	7.55	0.141
	TOS3	519.0	-3.60	1.40	0.556	13.10	0.034
V_{cmax}^{25}							
	TOS1	---	---	16.69	0.002	20.39	-0.001
	TOS2	---	---	19.42	0.003	**6.05**	0.003
	TOS3	---	---	18.95	0.002	8.14	0.002

For each trait-trait relationship, significantly different slopes or intercepts of TOS2 or TOS3 from TOS1 are indicated in bold. ---, not estimated.

Supplementary Table S10. **2018:** Parameter estimates of regression models of leaf functional traits (net CO_2 assimilation rate, A^{25}; rate of CO_2 efflux, $R_{dark}\_CO_2^{25}$; and rate of O_2 consumption, $R_{dark}\_O_2^{25}$) with leaf mass per unit area (LMA) or leaf N concentration grouped by time of sowing (TOS). Estimates are given for trait-trait relationships on an area or mass basis.

Structural or chemical traits		Area-based functional leaf traits					
		A^{25}		$R_{dark}\_CO_2^{25}$		$R_{dark}\_O_2^{25}$	
		Intercept	Slope	Intercept	Slope	Intercept	Slope
LMA							
	TOS1	7.37	0.20	0.29	0.019	0.14	0.011
	TOS2	20.10	**-0.19**	1.46	0.004	0.64	0.001
	TOS3	3.71	0.18	0.61	0.013	0.32	0.008
N							
	TOS1	9.10	38.40	0.52	3.479	0.85	-0.117
	TOS2	**19.58**	**-44.00**	**1.67**	0.030	0.23	2.110
	TOS3	4.03	49.40	0.68	3.480	0.47	1.370
V_{cmax}^{25}							
	TOS1	---	---	1.91	-0.003	0.81	0.000
	TOS2	---	---	1.54	0.001	0.95	-0.001
	TOS3	---	---	1.44	-0.001	0.62	0.001
		Mass-based functional leaf traits					
		A^{25}		$R_{dark}\_CO_2^{25}$		$R_{dark}\_O_2^{25}$	
		Intercept	Slope	Intercept	Slope	Intercept	Slope
LMA							
	TOS1	332.8	-0.49	19.0	0.073	15.08	-0.033
	TOS2	540.0	**-6.59**	**62.2**	**-0.550**	21.58	-0.156
	TOS3	315.0	-1.25	32.5	-0.150	18.20	-0.087
N							
	TOS1	529.0	-6.24	24.2	-0.018	6.10	0.187
	TOS2	475.0	-7.58	33.7	-0.089	25.61	-0.325
	TOS3	121.0	3.17	10.2	0.359	22.21	-0.227
V_{cmax}^{25}							
	TOS1	---	---	24.9	-0.001	13.18	0.000
	TOS2	---	---	26.9	0.001	16.47	-0.001
	TOS3	---	---	26.4	-0.001	13.29	0.000

For each trait-trait relationship, significantly different slopes or intercepts of TOS2 or TOS3 from TOS1 are indicated in bold.

Table S11. Regression coefficients (r^2) for leaf trait-trait relationships with data combined for 2017 and 2018.

Structural or chemical traits	Area based functional traits			Mass based functional traits		
	A^{25}	$R_{dark}\_CO_2^{25}$	$R_{dark}\_O_2^{25}$	A^{25}	$R_{dark}\_CO_2^{25}$	$R_{dark}\_O_2^{25}$
LMA	0.22***	0.11***	0.03*	0.00^{ns}	0.10***	0.04**
N	0.20***	0.00^{ns}	0.09***	0.02*	0.09***	0.04*
V_{cmax}^{25}	---	0.00^{ns}	0.02^{ns}	---	0.02^{ns}	0.01^{ns}
LMA+N	0.26***	0.14***	0.12***	0.02^{ns}	0.15***	0.09***
LMA+N+V_{cmax}^{25}	---	0.15***	0.10***	---	0.10***	0.10***

A^{25} (μmol CO_2 m^{-2} s^{-1}), net CO_2 assimilation rate measured at 25°C; $R_{dark}\_CO_2^{25}$ (μmol CO_2 m^{-2} s^{-1}), dark respiration (CO_2 efflux) rate measured at 25°C; $R_{dark}\_O_2$ (μmol O_2 m_{LA}^{-2} s^{-1}), dark respiration (O_2 consumption); LMA (g m^{-2}), leaf mass per unit area; Leaf N expressed on either area basis (g m^{-2}) or mass basis (mg gDM^{-1}); V_{cmax}^{25}, maximum carboxylation capacity of photosynthetic capacity at 25°C (μmol CO_2 m^{-2} s^{-1}). ---, not estimated. ^{ns}=not significant. *$P < 0.05$. **$P < 0.01$. ***$P < 0.001$.